Recent Heavy Flavor results from ATLAS

Yue Xu
University of Washington

IHEP EPD seminar

17th Dec, 2024

ATLAS EXPERIMENT

UNIVERSITY of WASHINGTON

The Large Hadron Collider

- The largest particle collider in the world
  - 27km circumference
  - Four major experiments: CMS, LHCb, **ATLAS**, ALICE

The ATLAS detector

- General-purpose detector
- Designed in layers to observe different types of particles
- Cumulative luminosities
    - Run 2 (2015-2018): 140fb^{-1} (physics)
    - Run3 (2022-): 183fb^{-1} (recorded)

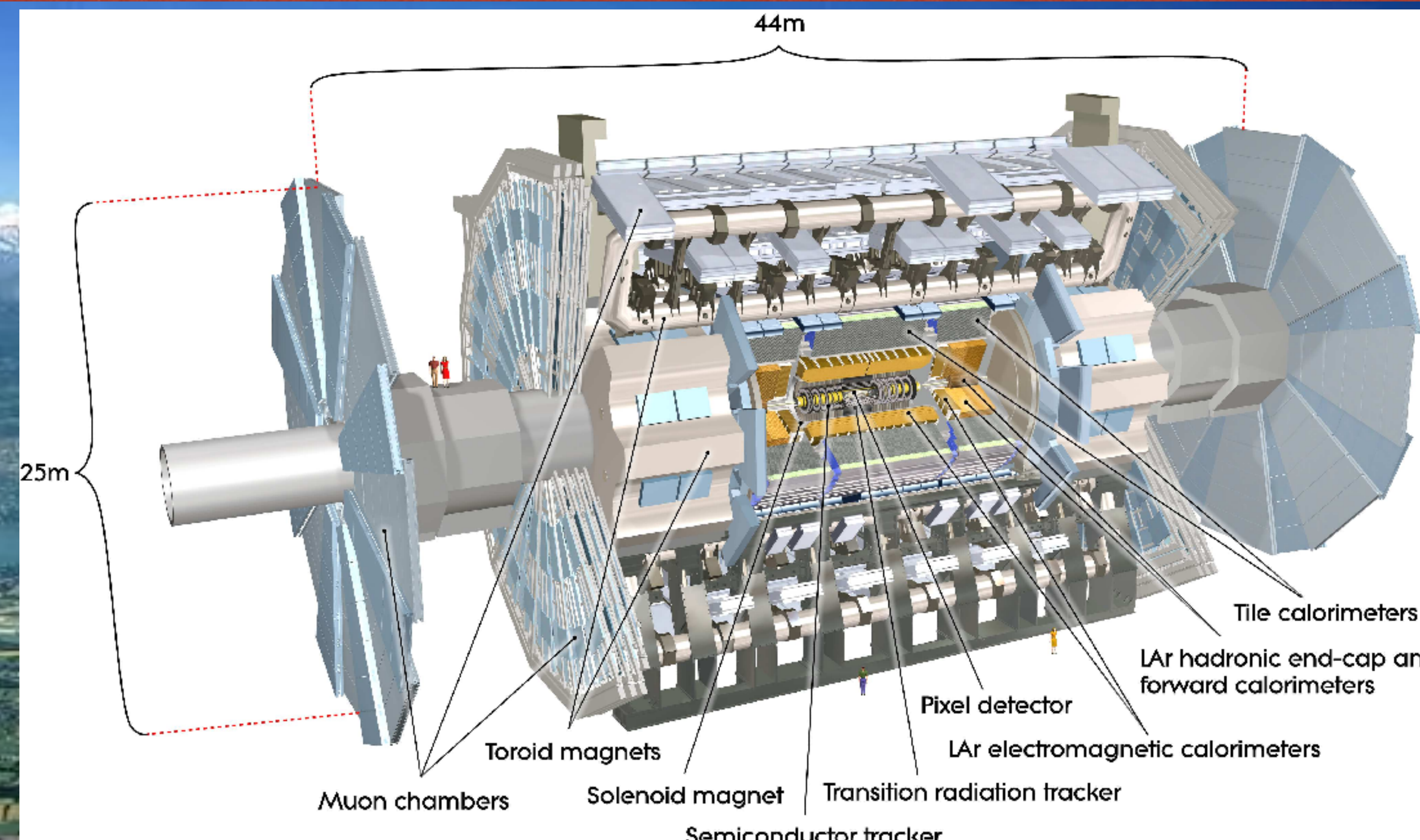

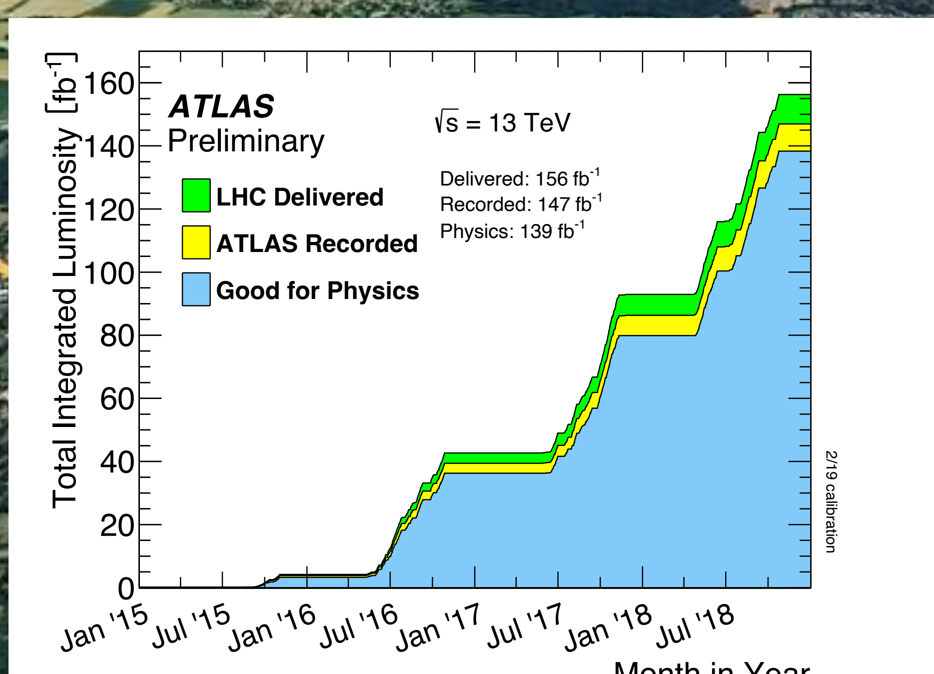

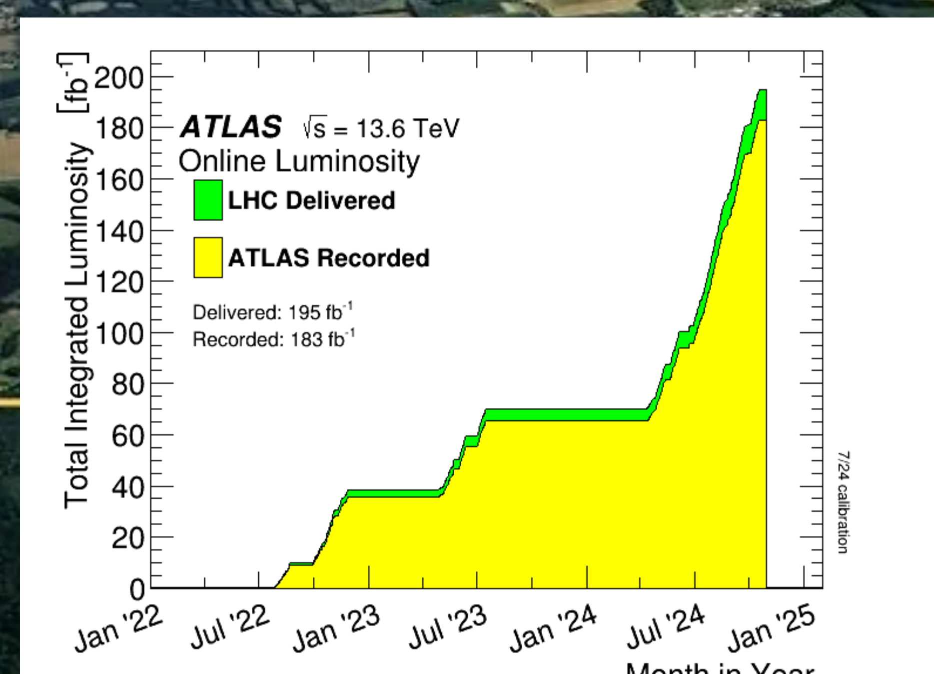

The ATLAS Pixel detector

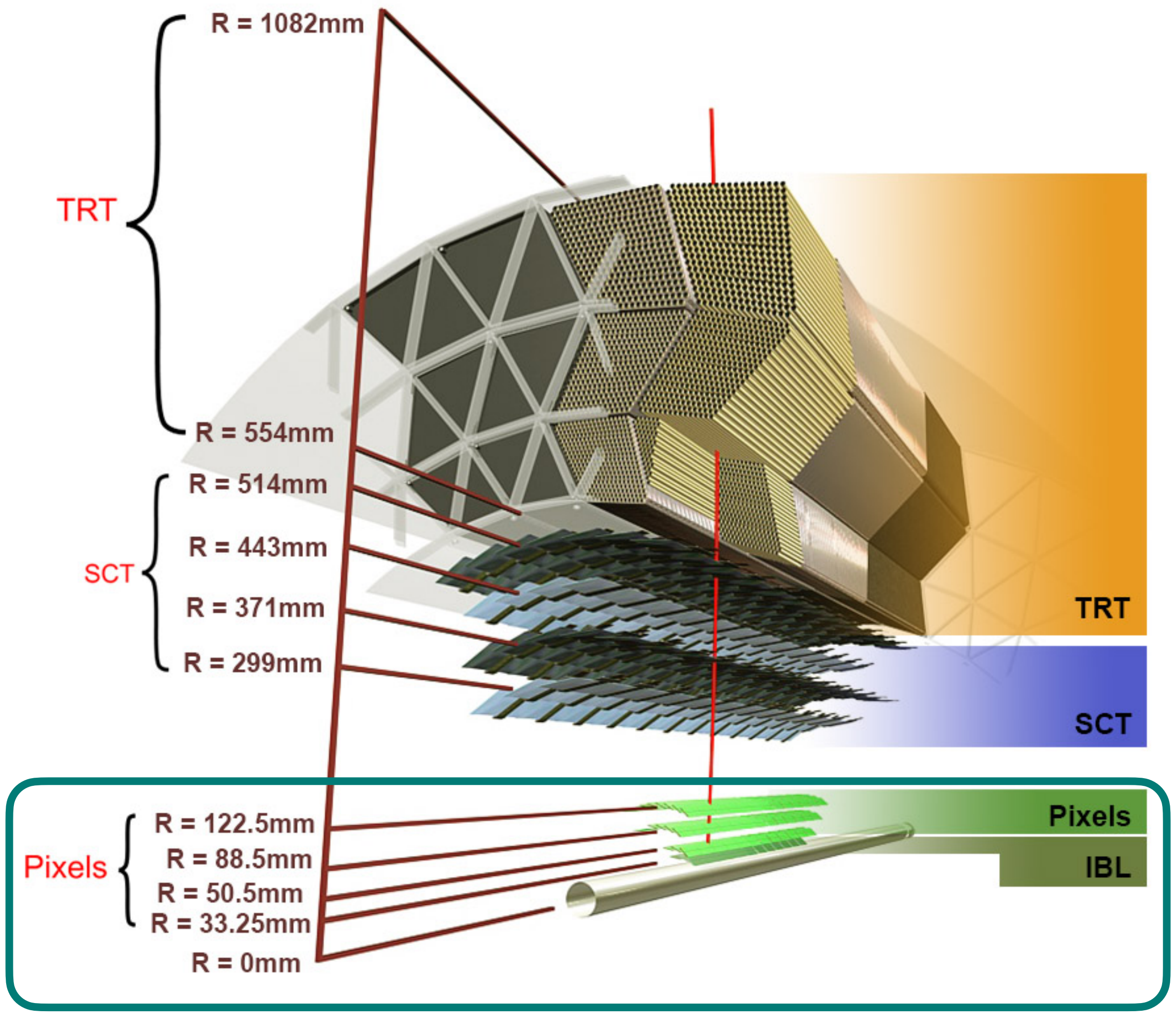

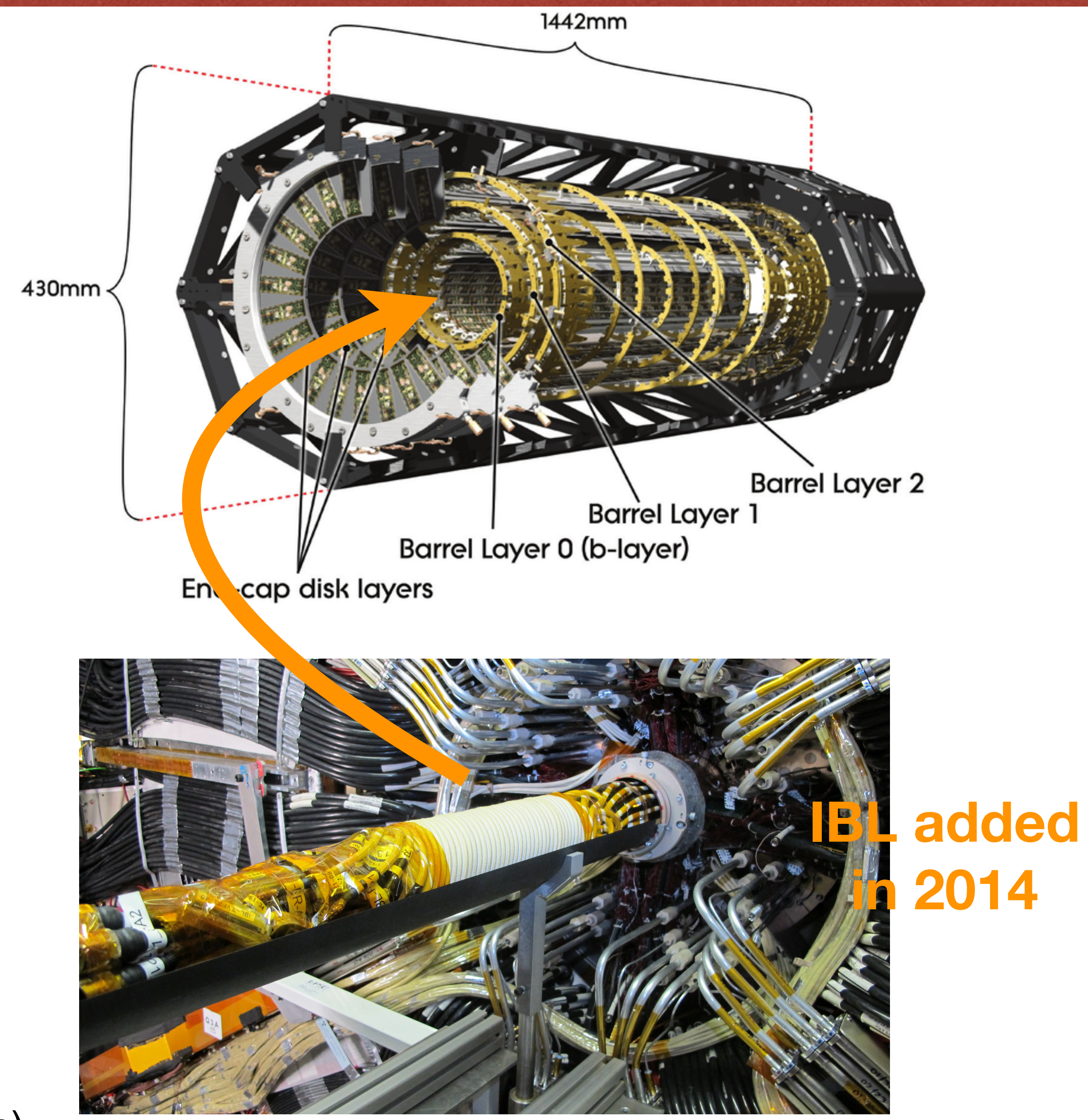

- Pixels: 3 barrel layers + 3 end-cap disks (per side)
  - Operating since 2008
- Insertable B-Layer (IBL): inserted during the first long LHC shutdown (2013-2014)
  - Operating since 2015
  - Five times better rejection of b-tagging than Run 1

Pixel performance in 2024

- 0.1% deadtime contribution (0.3% in 2023)
- Stable running without major issues, even with higher pile-up
  - Thanks to lots of hardware maintance, and improvements on software and firmware

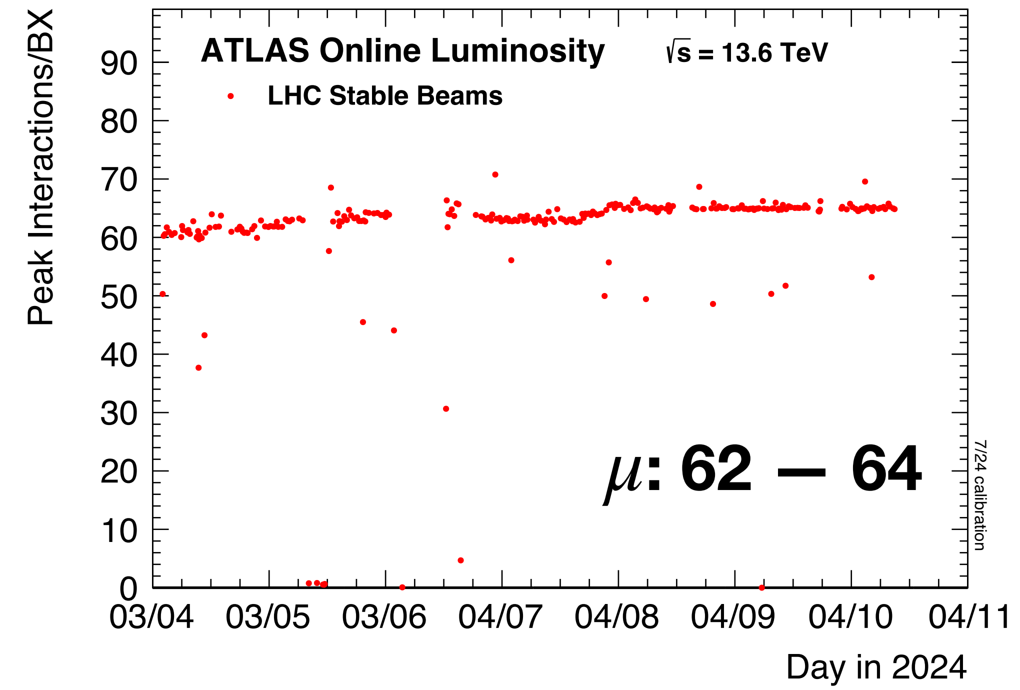

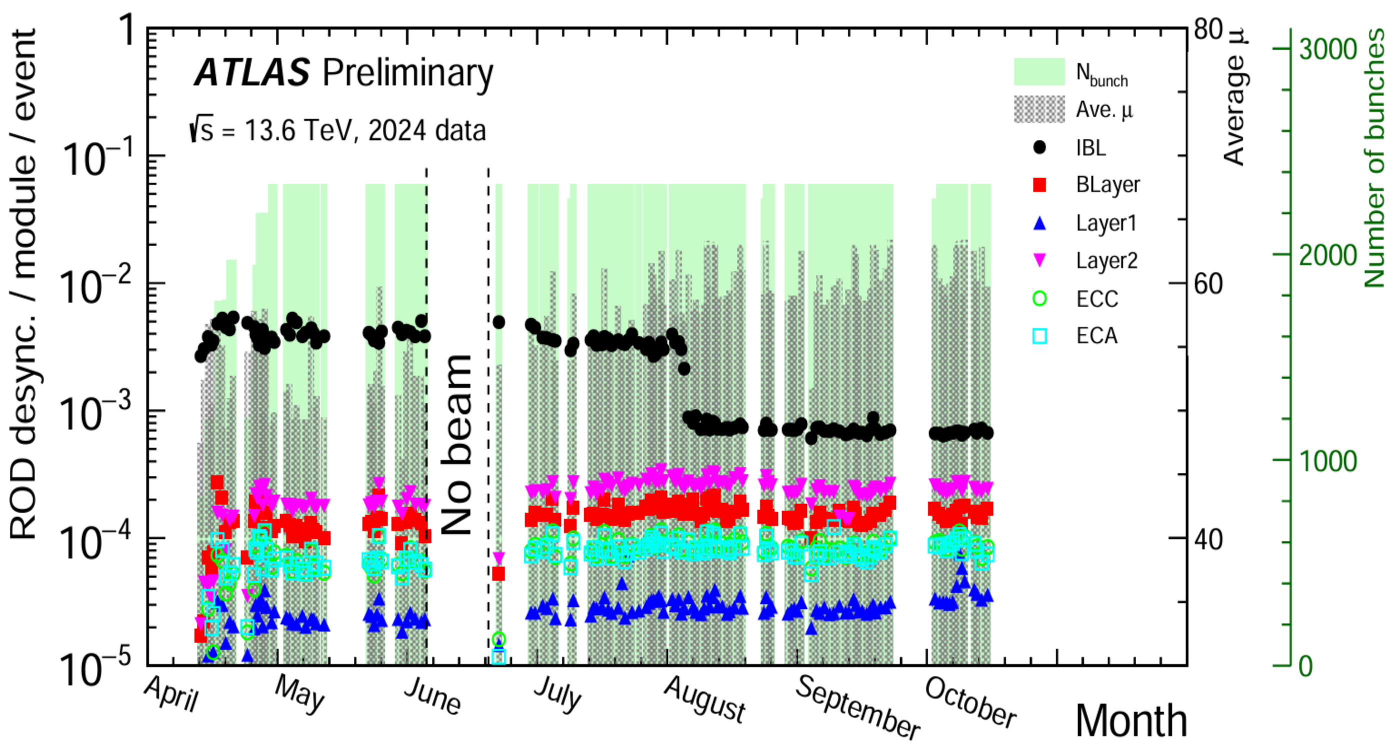

B physics in ATLAS

- Analyses focus mostly on final states with muons
- Dedicated B-physics triggers
- Excellent track and muon identification with the goodness of the inner detector and muon spectrometer

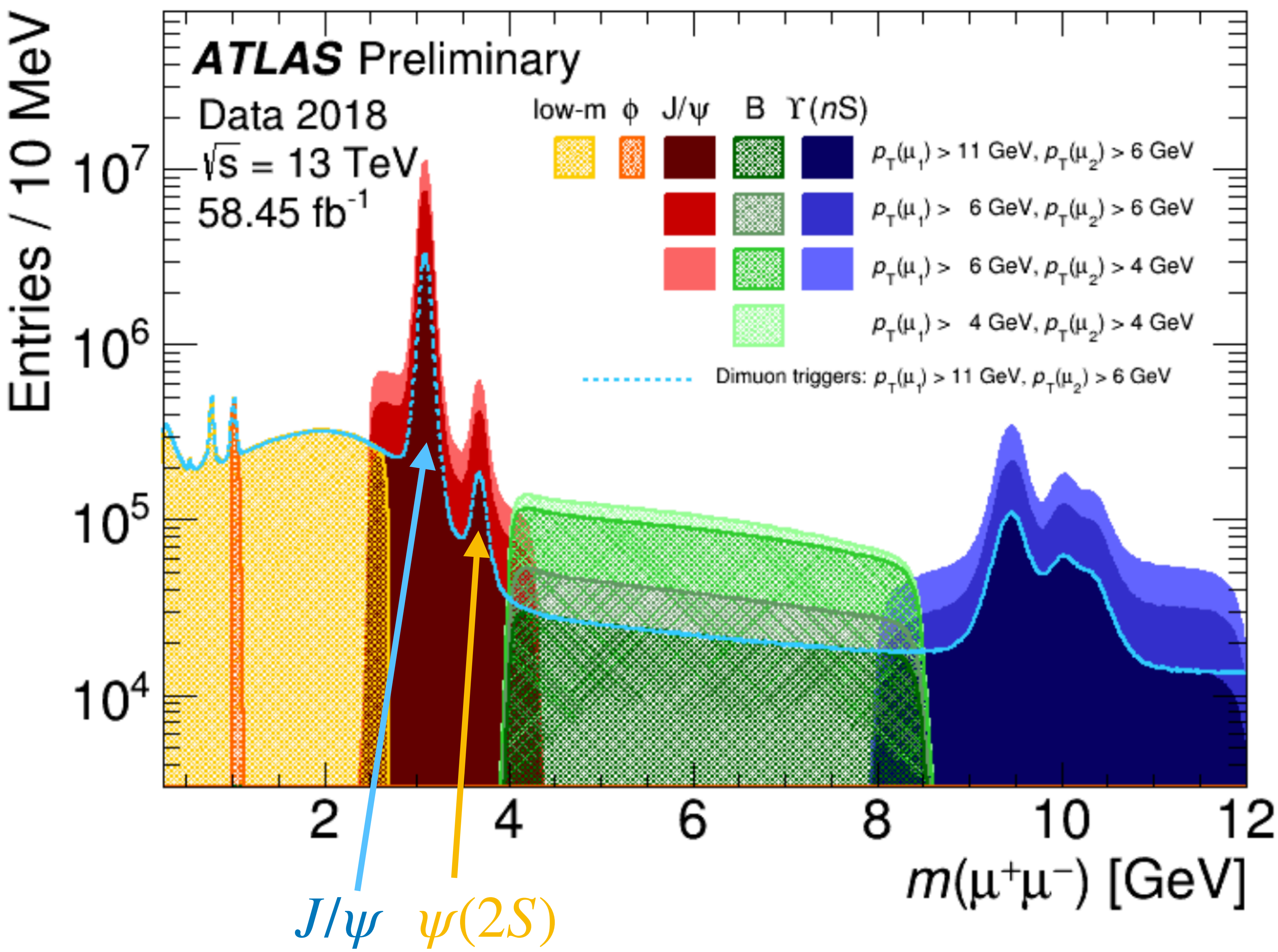

In this talk

- B^0 meson lifetime measurement
- Cross-section measurement of J/ψ and $\psi(2S)$ mesons
- Di-charmonium resonances

ATLAS full run 2 (2015-2018) data with a luminosity of 140fb^{-1} are used

B^0 meson lifetime measurement

arXiv:2411.09962

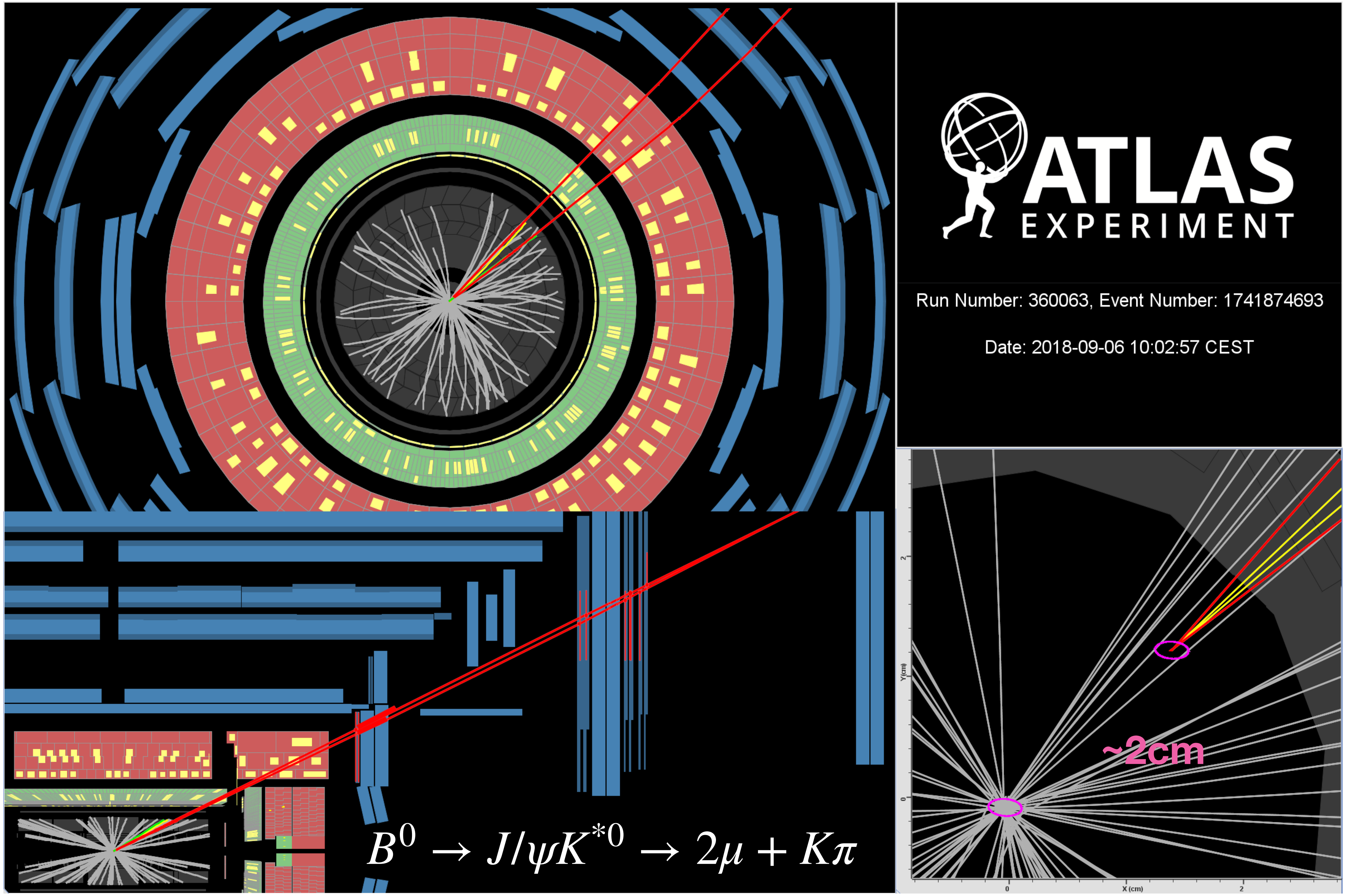

Introduction

- Studies on b-hadron lifetimes test our understanding of the weak interaction
- In the heavy-quark expansion (HQE) framework, the total decay rate $\Gamma = 1/\tau$ of a weekly decay heavy hadron B_q can be calculated by

$$\Gamma(\mathscr{B}_q) = \Gamma_3 + \delta\Gamma(\mathscr{B}_q)$$

leading

Free b-quark decay:

\+ free of non-perturbative uncertainties

0 Looks like the muon decay

$$\Gamma_3 \propto \frac{G_F^2 m_b^5}{192\pi^3} V_{cb}^2$$

\- Quark masses are difficult to define, huge dependence on definition can be reduced by higher order **perturbative corrections**

subleading

Power-suppressed terms on the HQE:

\+ suppressed with at least 2 powers of $1/m_b \Rightarrow$ small

0 Individual contributions are products of **perturbative** Wilson coefficients and **non-perturbative matrix elements** (determined with lattice-QCD, sum rules and/or from fits of experimental data of inclusive semi-leptonic decays - V_{cb})

JHEP01(2023)004

  - Predicted $\Gamma_d = 0.63^{+0.11}_{-0.07}$ ps^{-1}, large theoretical uncertainties due to m_b^5 in Γ_3
  - Predicted $\Gamma_d/\Gamma_s = 1.003 \pm 0.006$, smaller uncertainties as Γ_3 cancels out
- Lifetimes can also be used to test new physics models:

$$\Gamma(\mathscr{B}_q) = \Gamma_3^{\mathrm{SM}} + \Gamma_3^{\mathrm{BSM}} + \delta\Gamma(\mathscr{B}_q)^{\mathrm{SM}} + \delta\Gamma(\mathscr{B}_q)^{\mathrm{BSM}}$$

Motivation

- Effective lifetime τ_{B^0} measured in $B^0 \to J/\psi K^{*0}$ is related to Γ_L and Γ_H (decay widths of light and heavy mass eigenstates of the $B^0 - \bar{B}^0$ system:

$$\tau_{B^0} = \frac{1}{\Gamma_d} \frac{1}{1-y^2} (\frac{1 + 2Ay + y^2}{1 + Ay})$$

$\Gamma_d = (\Gamma_L + \Gamma_H)/2$, average decay width

$y = \Delta\Gamma_d/(2\Gamma_d) = (\Gamma_L - \Gamma_H)/(2\Gamma_d)$, normalised width difference

The asymmetry A depening on the amplitudes of final state R_L^f and R_H^f : $A = \frac{R_H^f - R_L^f}{R_H^f + R_L^f}$

- Experimental value of Γ_d can be extracted with measured τ_{B^0} and values of y and A from Heavy Flavour Averaging group (HFLAV)

- Decay width ratio Γ_d/Γ_s can then be calculated with ATLAS measured $\Gamma_s = 0.6703 \pm 0.0014(\text{stat.}) \pm 0.0018(\text{syst.})$ ps^{-1} from $B_s^0 \to J/\psi\phi$ Eur. Phys. J. C 81 (2021) 342

Reconstruction and selection

- Di-muon triggers with J/ψ mass window requirement
- $B^0 \to J/\psi K^{*0}$ reconstruction:
  - $J/\psi \to \mu^+\mu^-$: fit oppositely charged muon pairs to a common vertex, $\chi^2/N_{\text{dof}} < 10$
  - $K^{*0} \to K^+\pi^-$: consider both $K^+\pi^-$ and $K^-\pi^+$, and choose the one closer to K^{*0} mass from PDG
  - B^0 candidate: $J/\psi \to \mu^+\mu^-$ and $K^{*0} \to K^+\pi^-$ are fitted to a common vertex with J/ψ mass constraint. The candidate with smallest χ^2/N_{dof} is selected
- Primary vertex (PV) candicate: the one with smallest 3D impact parameter a_0 is used
  - a_0: minimum distance between PV and the line extrapolated from the reconstructed B^0 vertex in the direction of B^0 momentum
- For each B^0 candidate, the proper decay time t is determined:

$$t = \frac{L_{xy} m_B}{p_{T_B}}$$

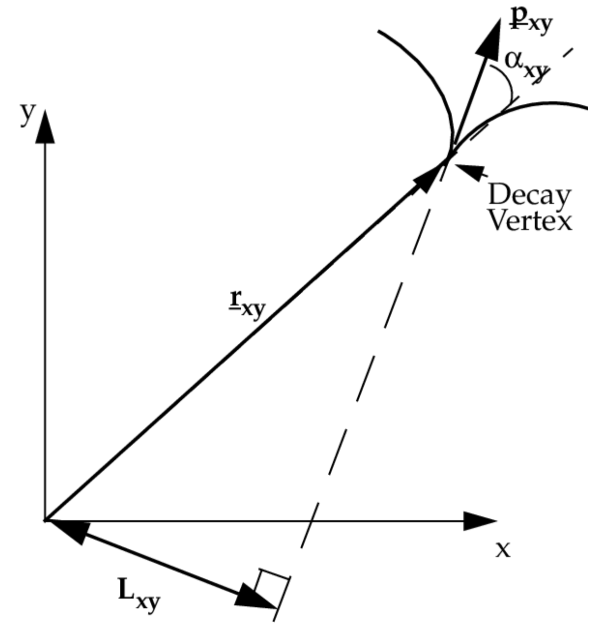

Fit model

- 2-dimensional unbinned maximum-likelihood fit on B^0mass and proper decay time is performed to extract B^0 lifetime:
  - Signal model: $B^0 \to J/\psi K^{*0}$ decay
  - Background model:
    - Prompt: J/ψ from $pp \to J/\psi X$ process combining with a random K^{*0}
    - Combinatorial: J/ψ from b-hadron decay combining with a random K^{*0}

$$\ln L = \sum_{i=1}^{N} w(t_i) \ln[f_{\mathrm{sig}} \mathcal{M}_{\mathrm{sig}}(m_i) \mathcal{T}_{\mathrm{sig}}(t_i, \sigma_{t_i}, p_{\mathrm{T}_i}) + (1 - f_{\mathrm{sig}}) \mathcal{M}_{\mathrm{bkg}}(m_i) \mathcal{T}_{\mathrm{bkg}}(t_i, \sigma_{t_i}, p_{\mathrm{T}_i})]$$

Signal mass probility density function (PDF) and time PDF

Background mass PDF and time PDF

$$P_{\mathrm{sig}}(t_i | \sigma_{t_i}, p_{\mathrm{T}_i}) = E(t', \tau_{B^0}) \otimes R(t' - t_i, \sigma_{t_i})$$

Uncertainties

Source of uncertainty	Systematic uncertainty [ps]
ID alignment	0.00108
Choice of mass window	0.00104
Time efficiency	0.00130
Best-candidate selection	0.00041
Mass fit model	0.00152
Mass-time correlation	0.00229
Proper decay time fit model	0.00010
Conditional probability model	0.00070
Fit model test with pseudo-experiments	0.00002
Total	0.0035

Statistical uncertainty: 0.0012 ps

- Systematic uncertainty dominates
  - Mass-time correlation, the correlation between invariant mass and the proper decay time, has the largest contribution

Mass and proper decay time

- The invariant mass and proper decay time projections of the fit
- B^0 signal events: 2450500 ± 2400

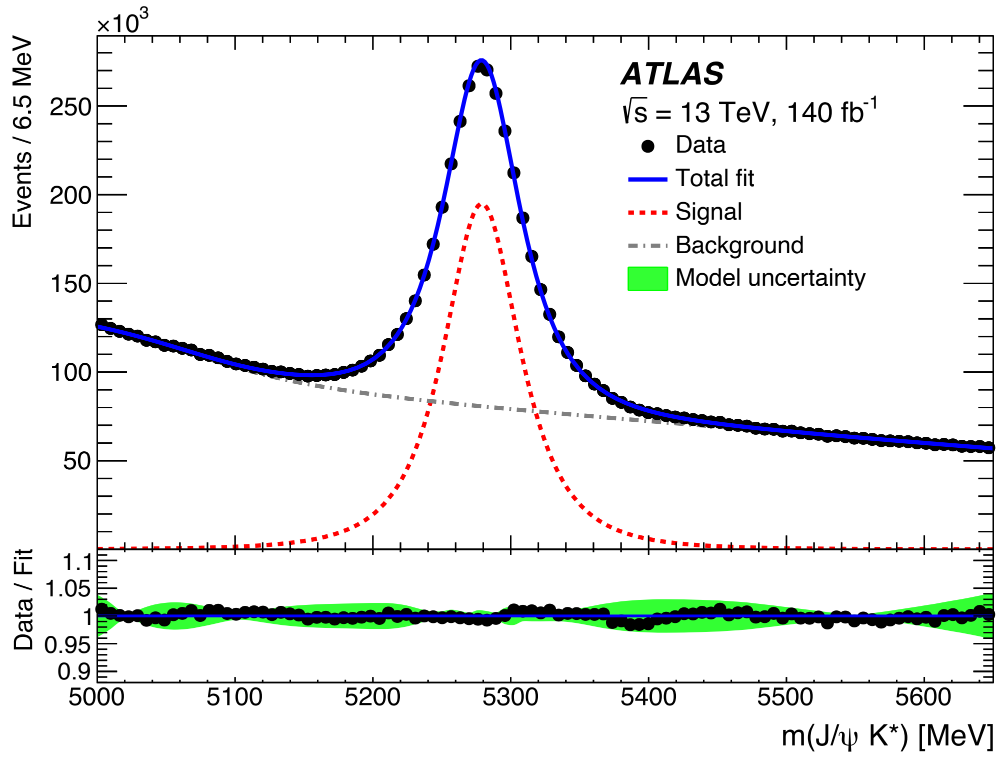

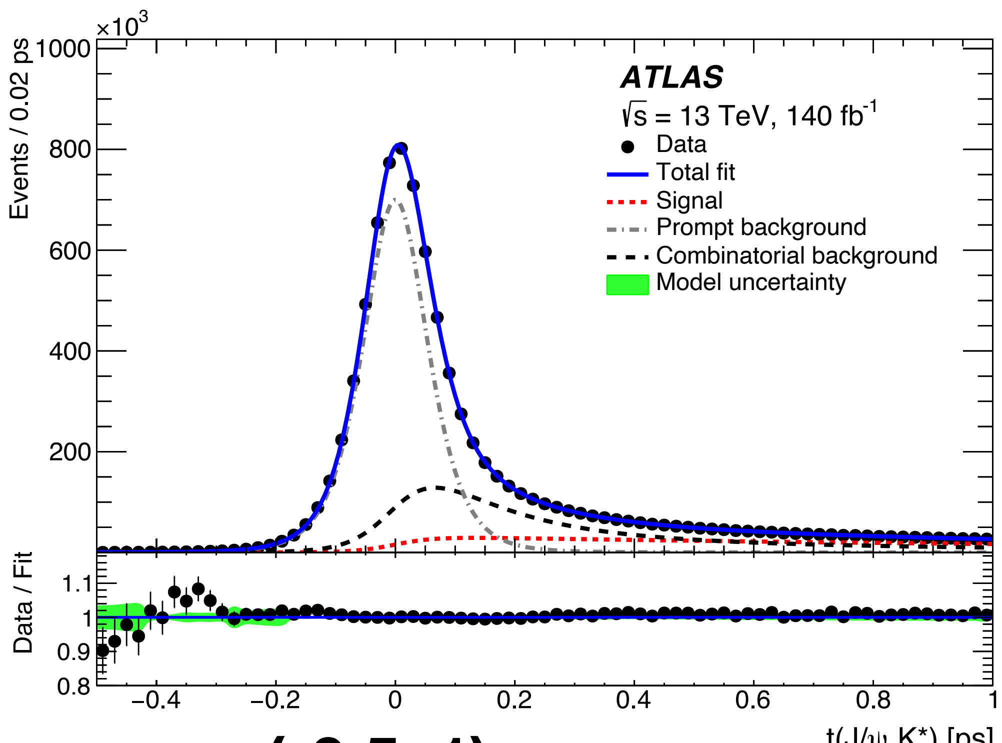

(-0.5, 1) ps

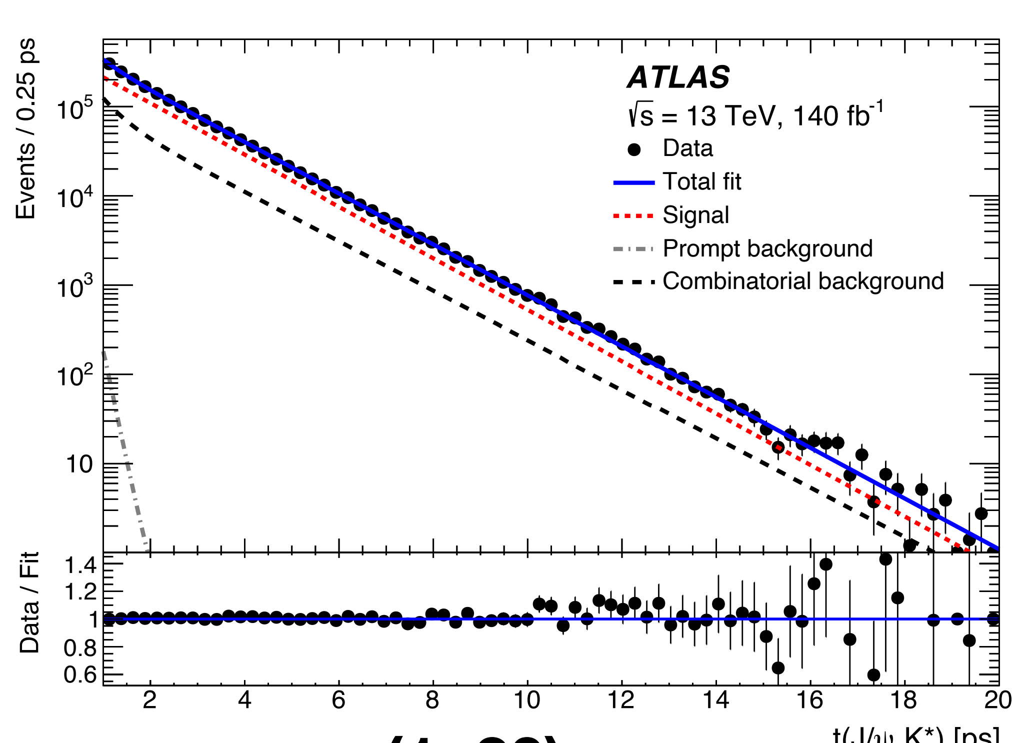

(1, 20) ps

Measured effective lifetime

- The measured B^0 effective lifetime is:

$$\tau_B^0 = 1.5053 \pm 0.0012(\textbf{stat.}) \pm 0.0035(\textbf{syst.})\ \textbf{ps}$$

- A consistency and stability test is performed with B^0 lifetime fitted separately for each data-taking period (2015+2016, 2017 and 2018)

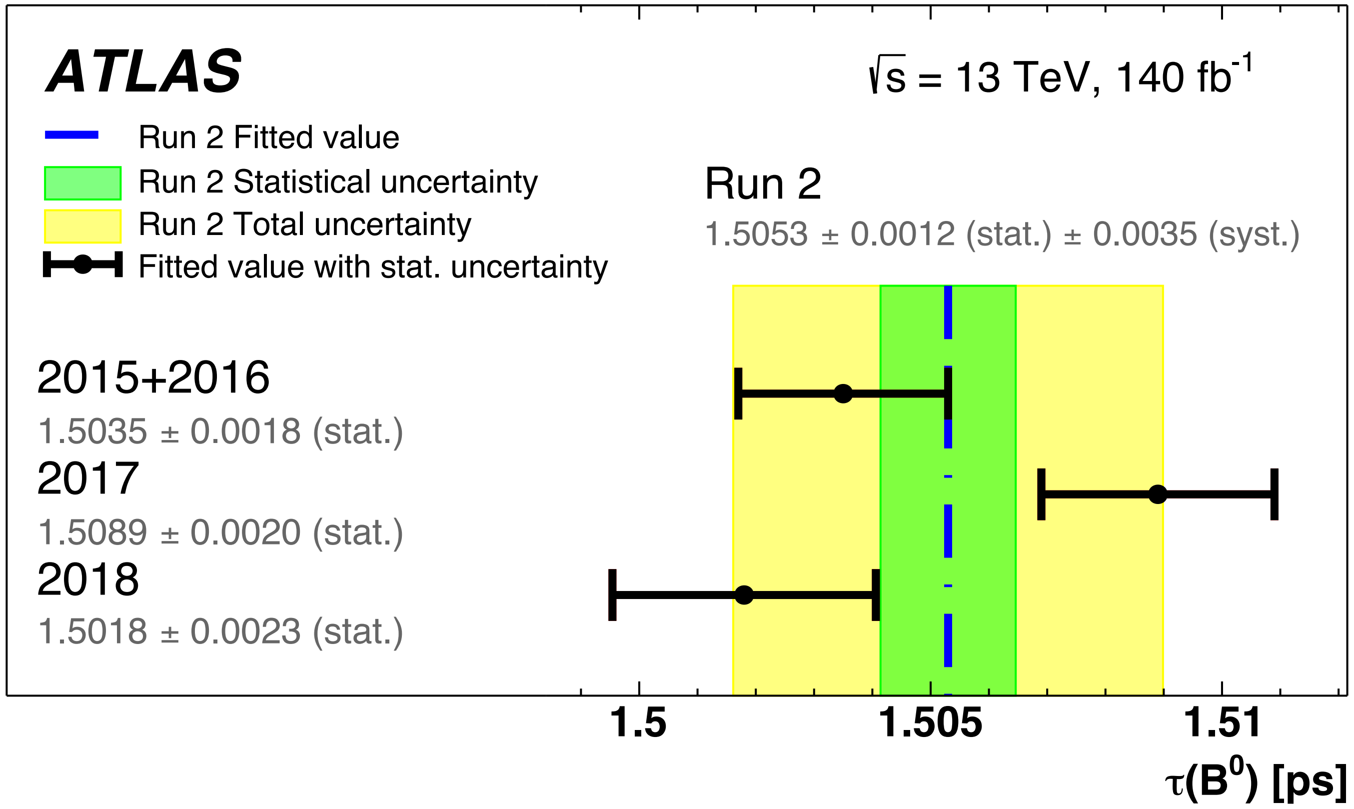

Compare to previous results

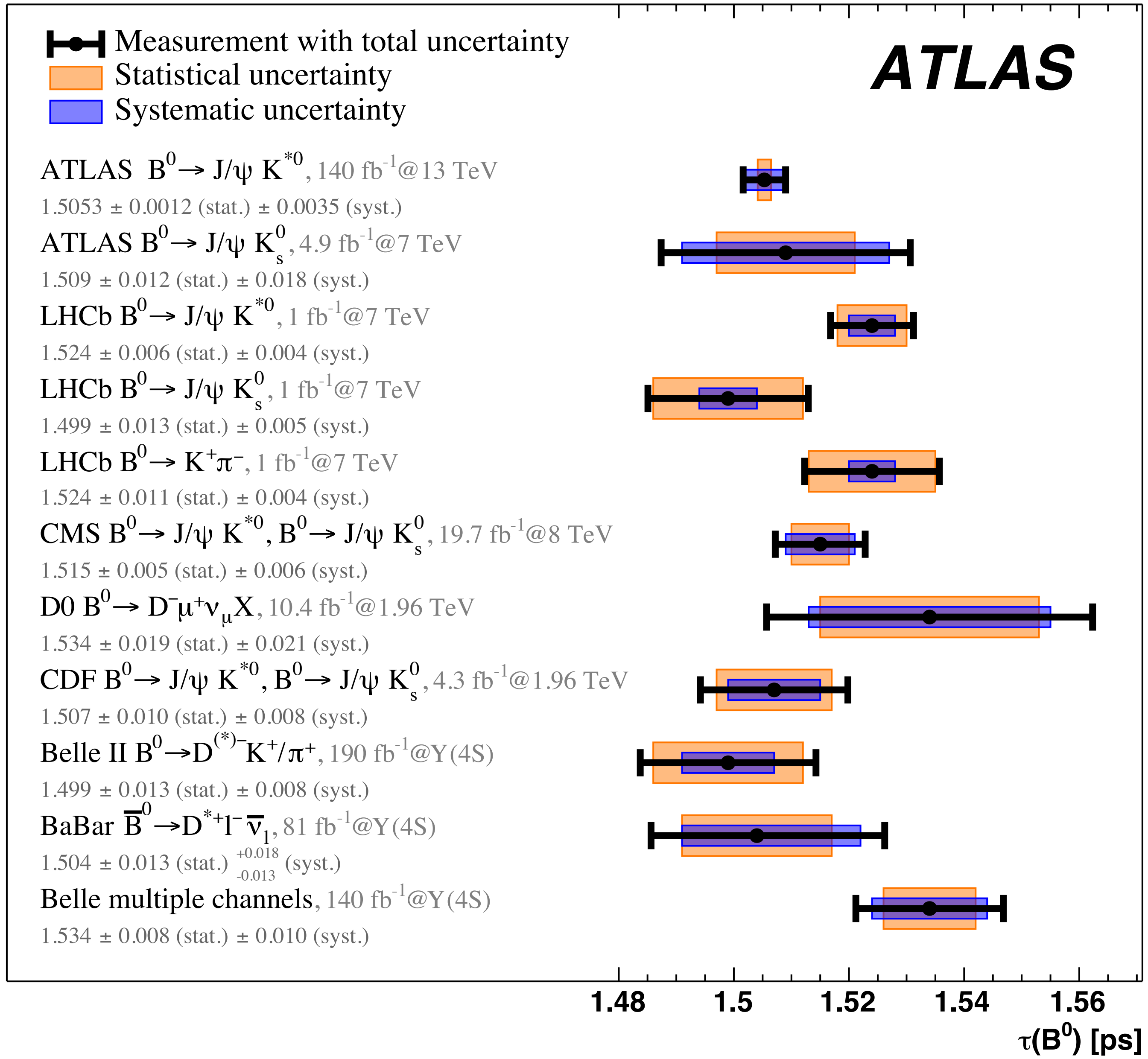

- ATLAS B^0 lifetime result is compitable with most of the other measurements
- Compare to the previous ATLAS results, the new measurement significantly reduces systematic uncertainty by a factor of ~4.7
  - Better vertexing after installing IBL

Γ_d and Γ_d/Γ_s

Γ_d

- Γ_d is extracted from measured τ_B^0 with input values $2y = \Delta\Gamma_d/\Gamma_d = 0.001 \pm 0.010$ and asymmetry $A = -0.578 \pm 0.136$ from HFLAV:

$$\tau_{B^0} = \frac{1}{\Gamma_d}\frac{1}{1-y^2}\left(\frac{1+2Ay+y^2}{1+Ay}\right)$$

$$\Gamma_d = 0.6639 \pm 0.0005(\textbf{stat.}) \pm 0.0016(\textbf{syst.}) \pm 0.0038(\textbf{ext.})\ \textbf{ps}^{-1}$$

- 'ext.' is the uncertainty originating from the HFLAV, calculated from uncertainties of y and A (dominant)
- Compitable with the HQE prediction of $0.63^{+0.11}_{-0.07}$ ps^{-1}

Γ_d/Γ_s

- Γ_d/Γ_s, ratio of the average decay widths of B^0 and B_s^0 mesons, is also extracted:

$$\Gamma_d/\Gamma_s = 0.9905 \pm 0.0022(\textbf{stat.}) \pm 0.0036(\textbf{syst.}) \pm 0.0057(\textbf{ext.})$$

- In agreement with theory predictions of HQE and lattice QCD models

Cross-section measurement of J/ψ and $\psi(2S)$ mesons

Eur. Phys. J. C 84 (2024) 169

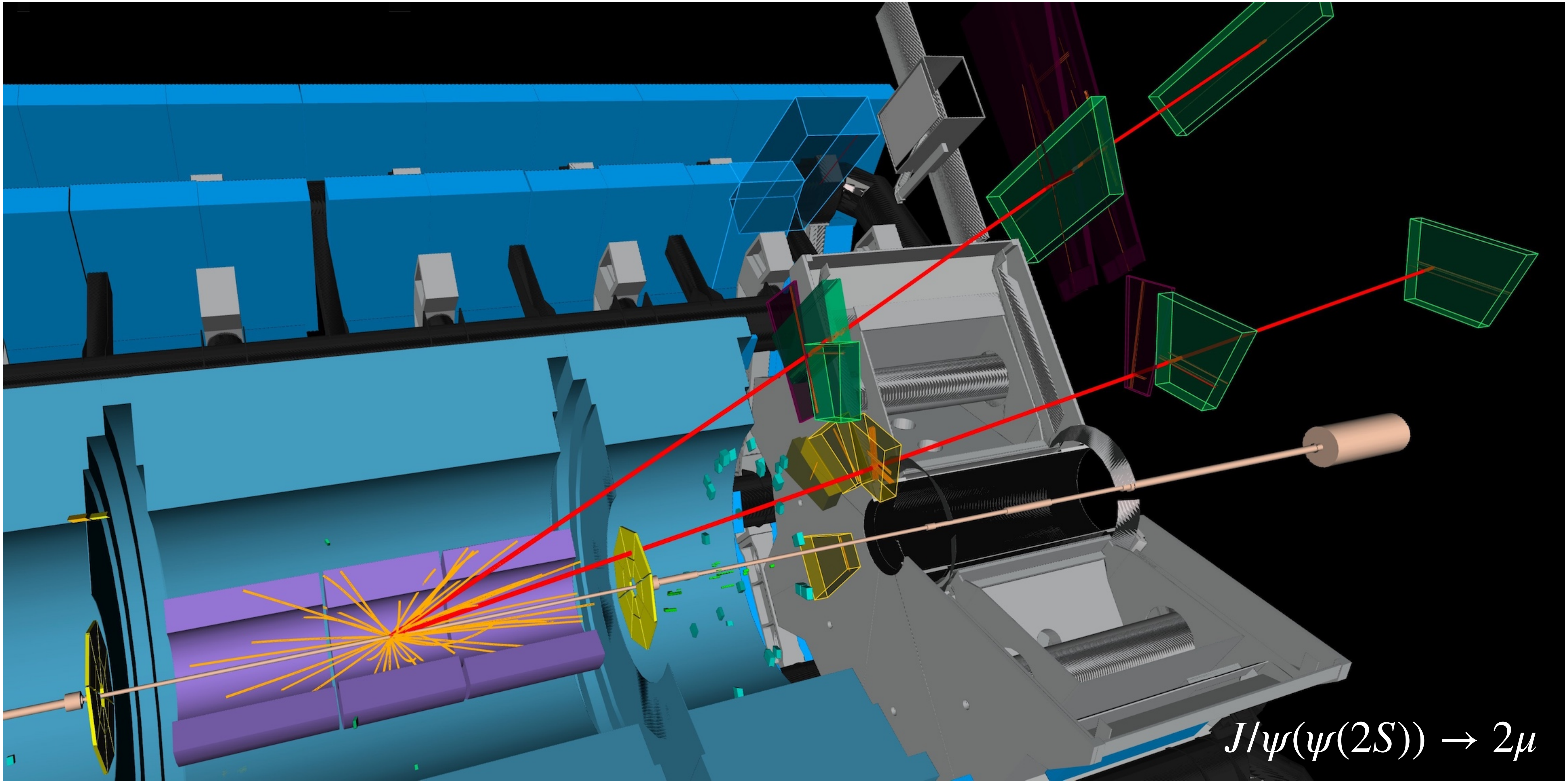

Introduction

- J/ψ and $\psi(2S)$ were discovered almost 50 years ago, but the QCD production mechanisms haven't been fully understood
  - Non-prompt production is well predicted by pQCD
  - Prompt production still needs to be understood
- Previous ATLAS measurement about J/ψ production exploited a di-muon trigger, with the high-pT reach limited mainly by the trigger performance to about 100 GeV (Run1 result: Eur. Phys. J. C 76 (2016) 283)
- New measurements of the J/ψ ($\psi(2S)$) meson production with full run-2 data, $140 \mathrm{fb}^{-1}$
  - Provide a much broader p_T coverage, **8-360 GeV** (**8-140 GeV**)
  - Combine di-muon trigger and single muon trigger
    - Di-muon trigger @ p_T threshold of 4 GeV (2.6 fb^{-1}), covering the region $8 < p_T^{di-\mu} < 60$ GeV
    - Single muon trigger @ p_T threshold of 50 GeV (140 fb^{-1}), covering the region $60 < p_T^{di-\mu} < 360(140)$ GeV

Di-muon spectrum

- A 2-dimensional unbinned maximum-likelihood fit is performed on di-muon mass and pseudo-proper decay time τ to obtain raw yields
- 34 di-muon p_T intervals and 3 |y| intervals

1.5 < |y| < 2
10 < p_T < 11 GeV

0.75 < |y| < 1.5
60 < p_T < 70 GeV

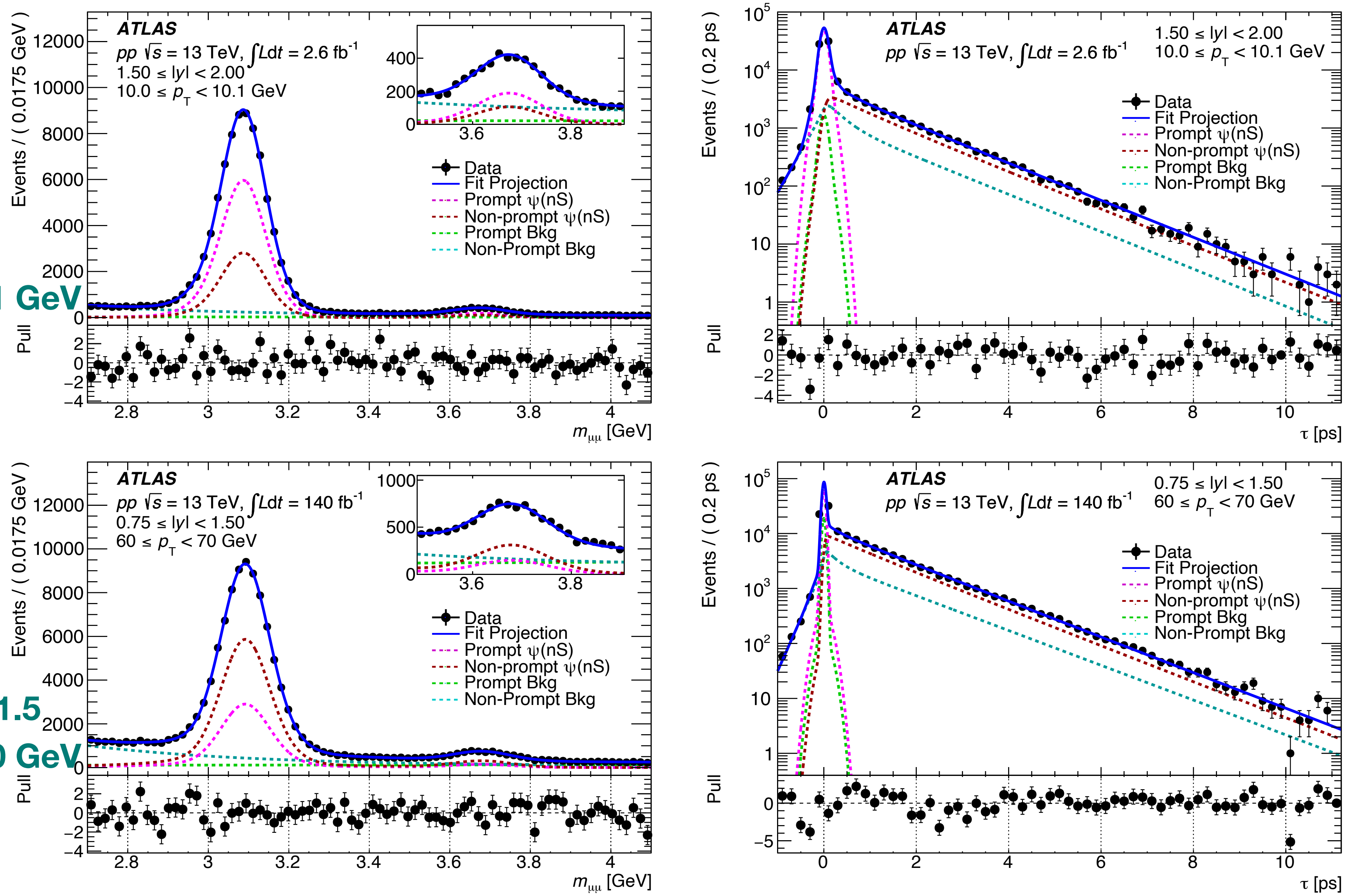

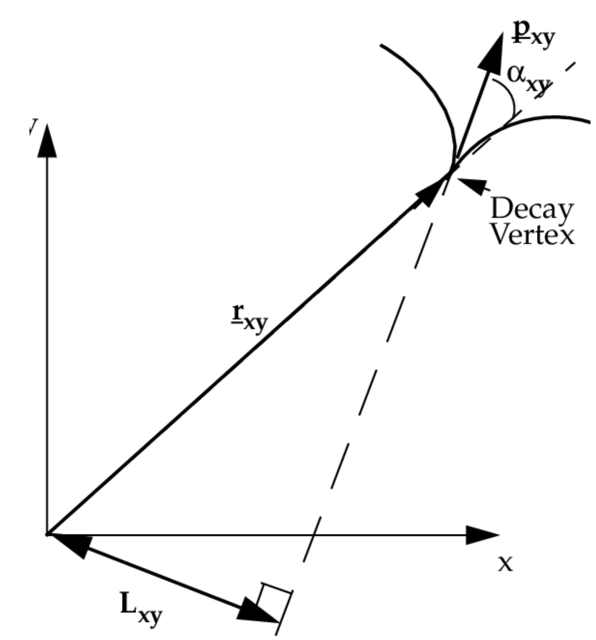

$$\tau = \frac{m}{p_T}\frac{L_{xy}}{c}$$

Uncertainties

- A variety of sources of systematic effects are studied:
  - Fit parameterisation
  - Muon reconstruction and trigger efficiencies
  - Acceptance corrections
- For corss section measurement, systematic uncertainty dominates
  - In low pT range, systematics on trigger and muon reconstruction have a larger impact
  - In high pT range, systematic from fit model dominates

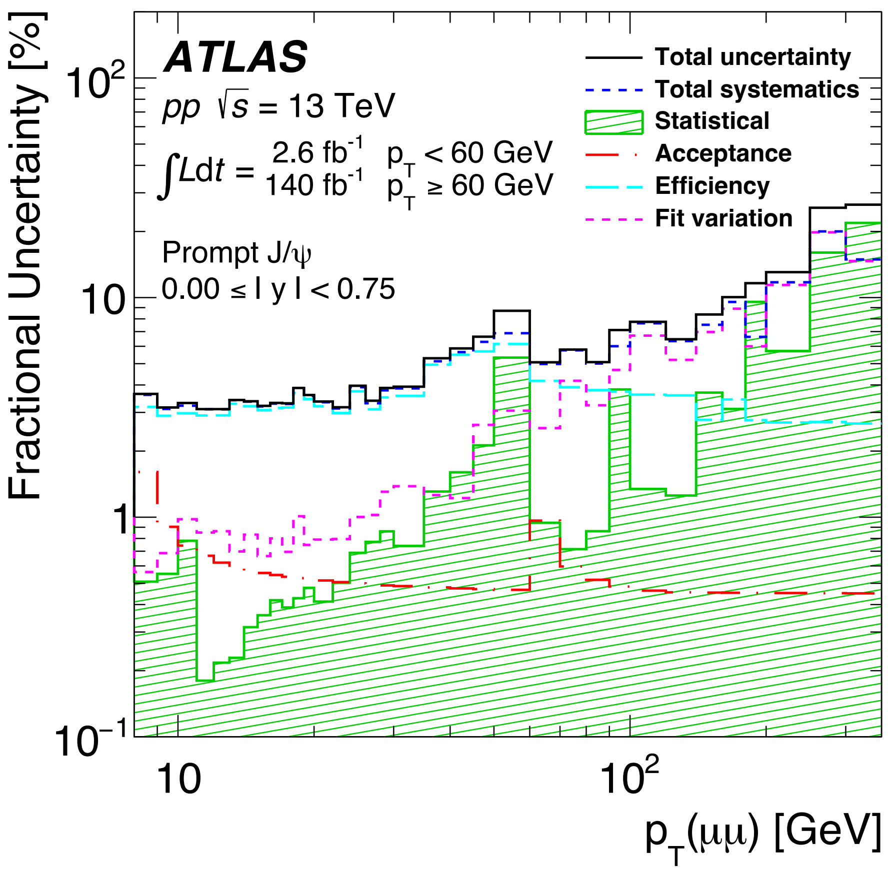

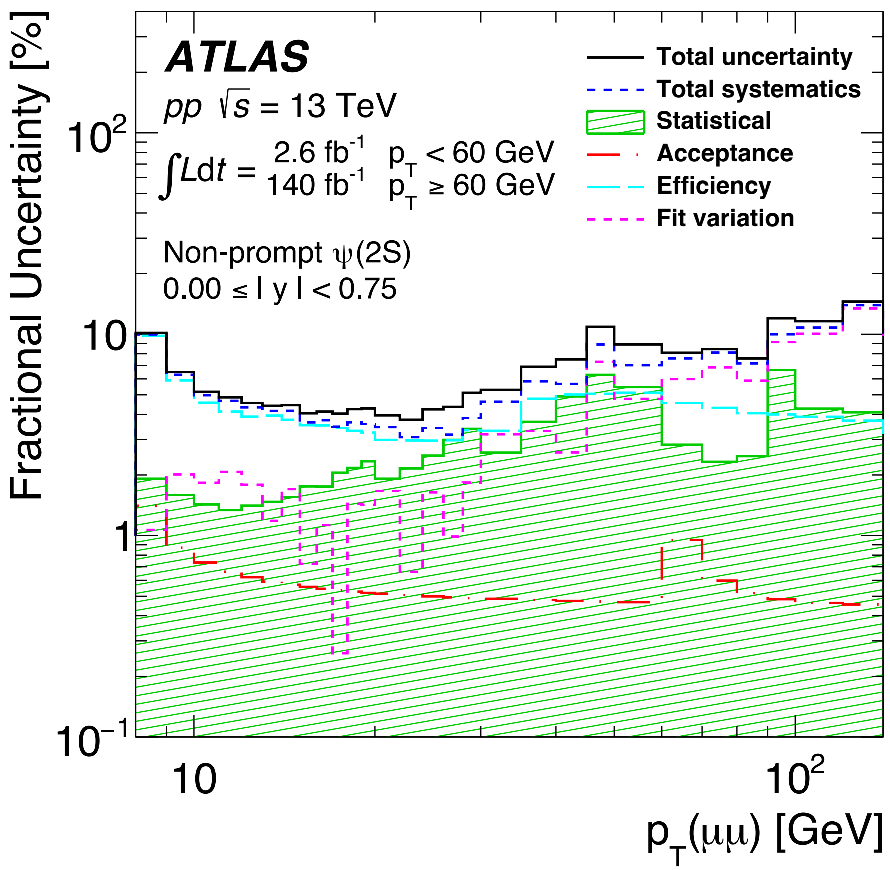

Uncertainties

- For non-prompt fractions and $\psi(2S)$-to-J/ψ ratios, statistical uncertainty dominate in many bins because the systematic uncertainties partially cancel out

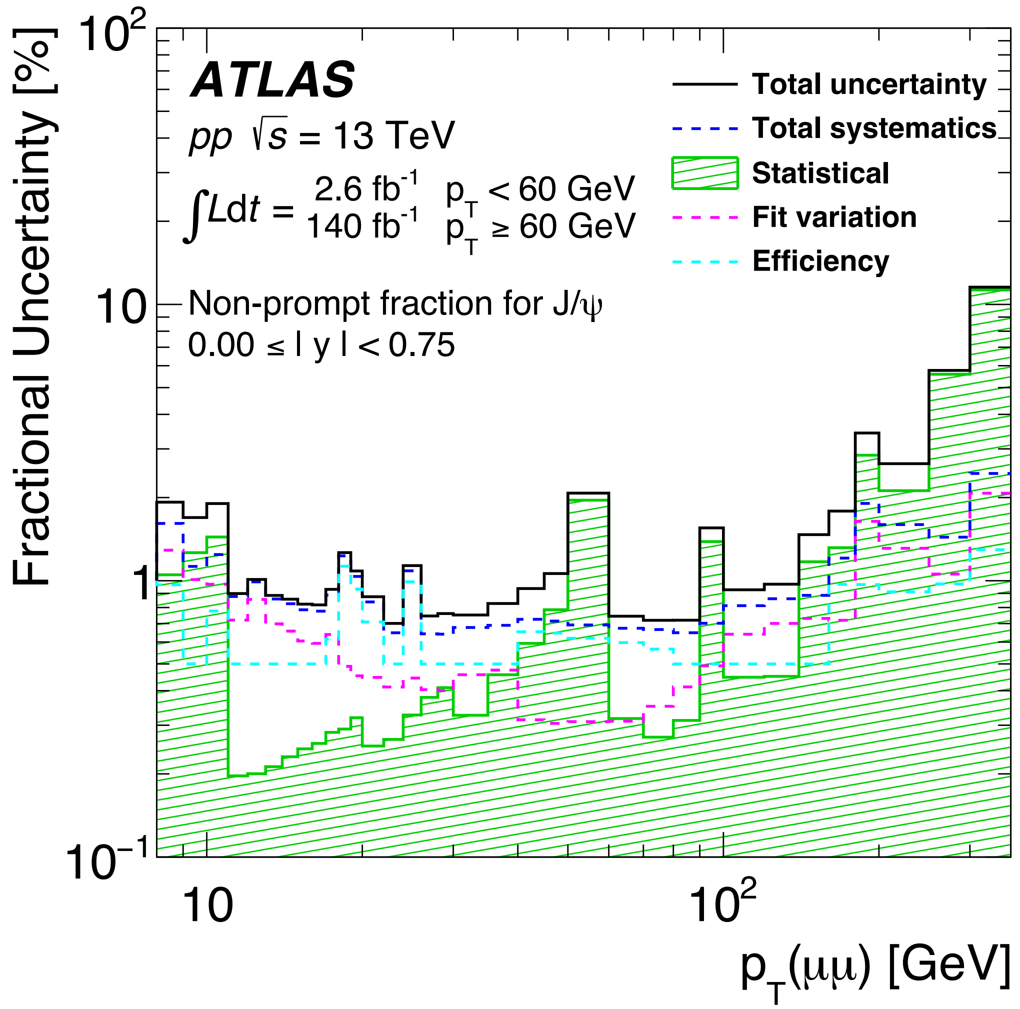

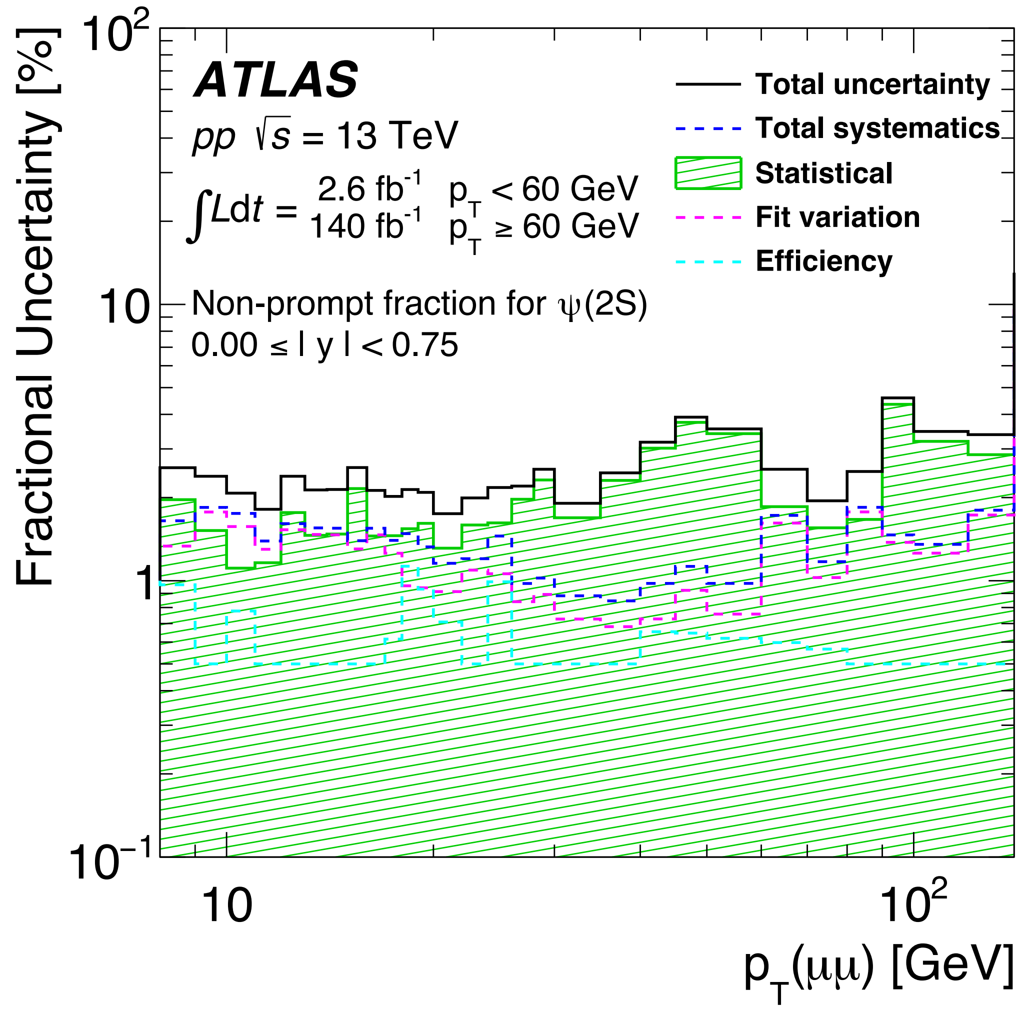

Cross-section measurements

- The measured double-differential cross-sections of prompt and non-prompt J/ψ ($\psi(2S)$) production
  - Prompt cross-sections are slightly larger at low p_T range

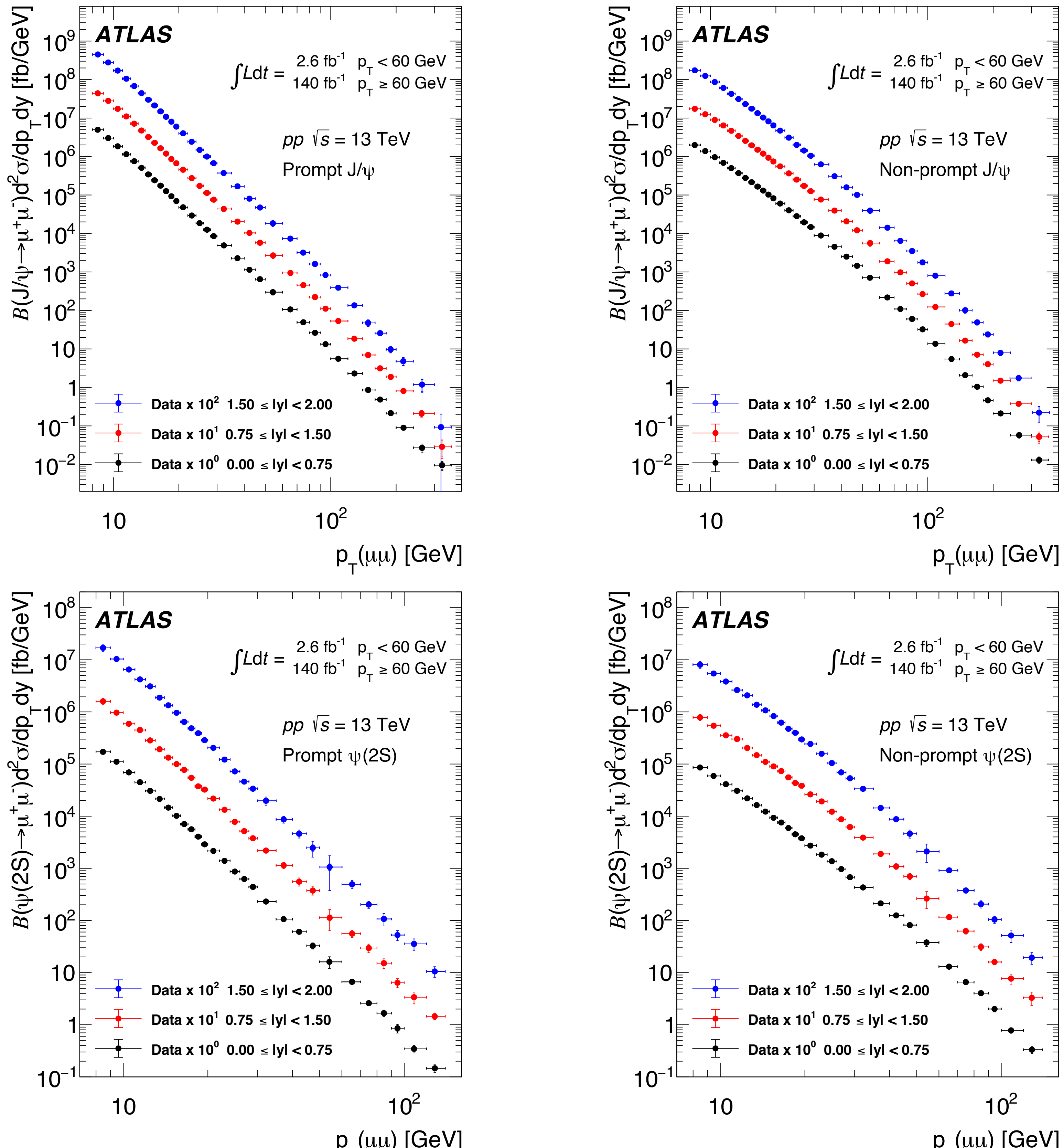

Non-prompt fraction

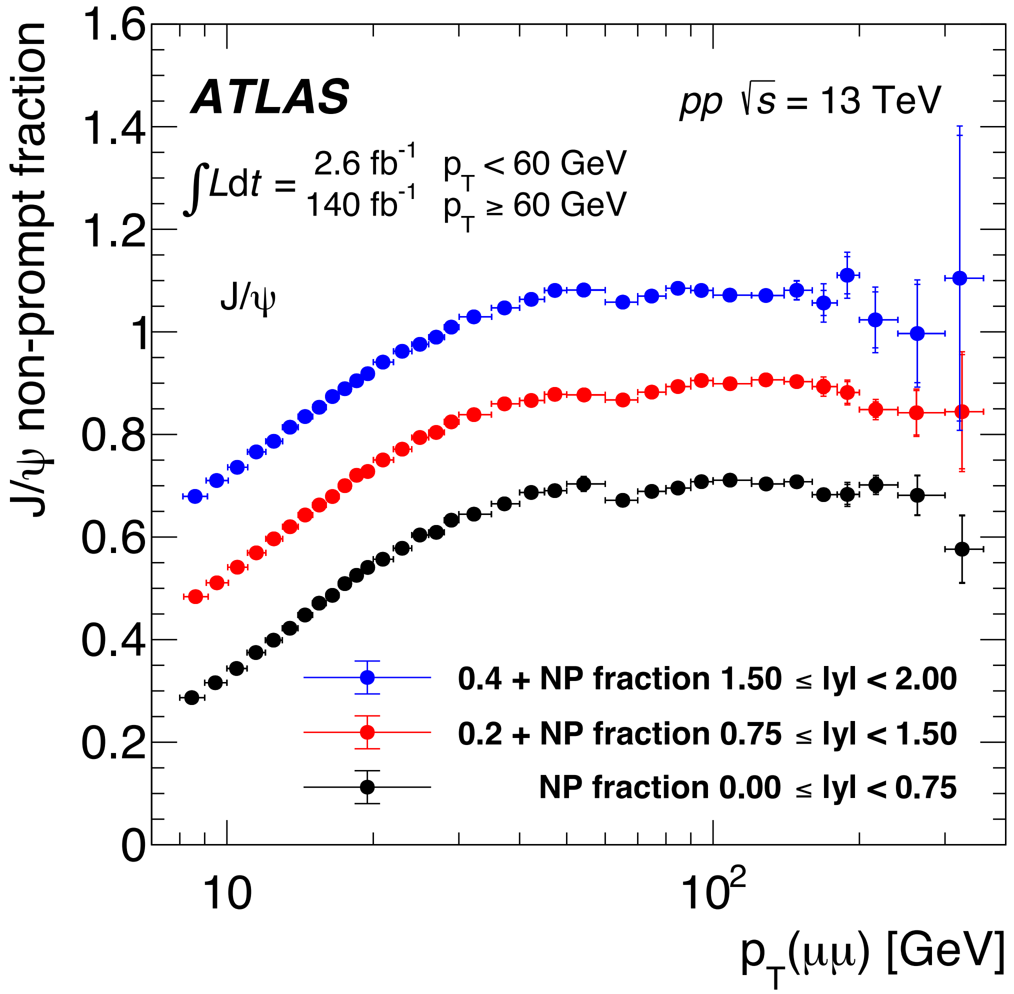

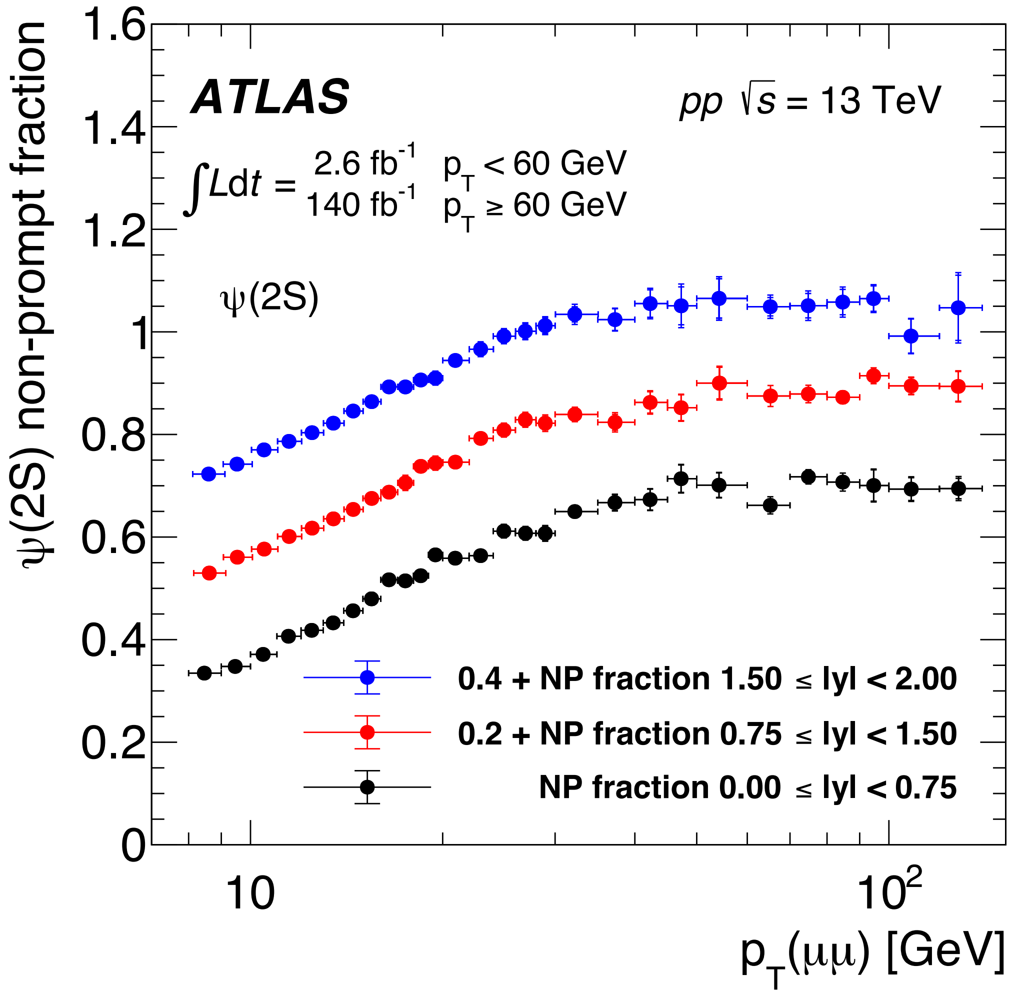

- Non-prompt fractions increase steadily with p_T up to 100 GeV
- Constant for both J/ψ and $\psi(2S)$ in the high p_T range
  - Similar p_T-dependences for prompt and non-prompt cross section at high p_T

$\psi(2S)$-to-J/ψ ratio

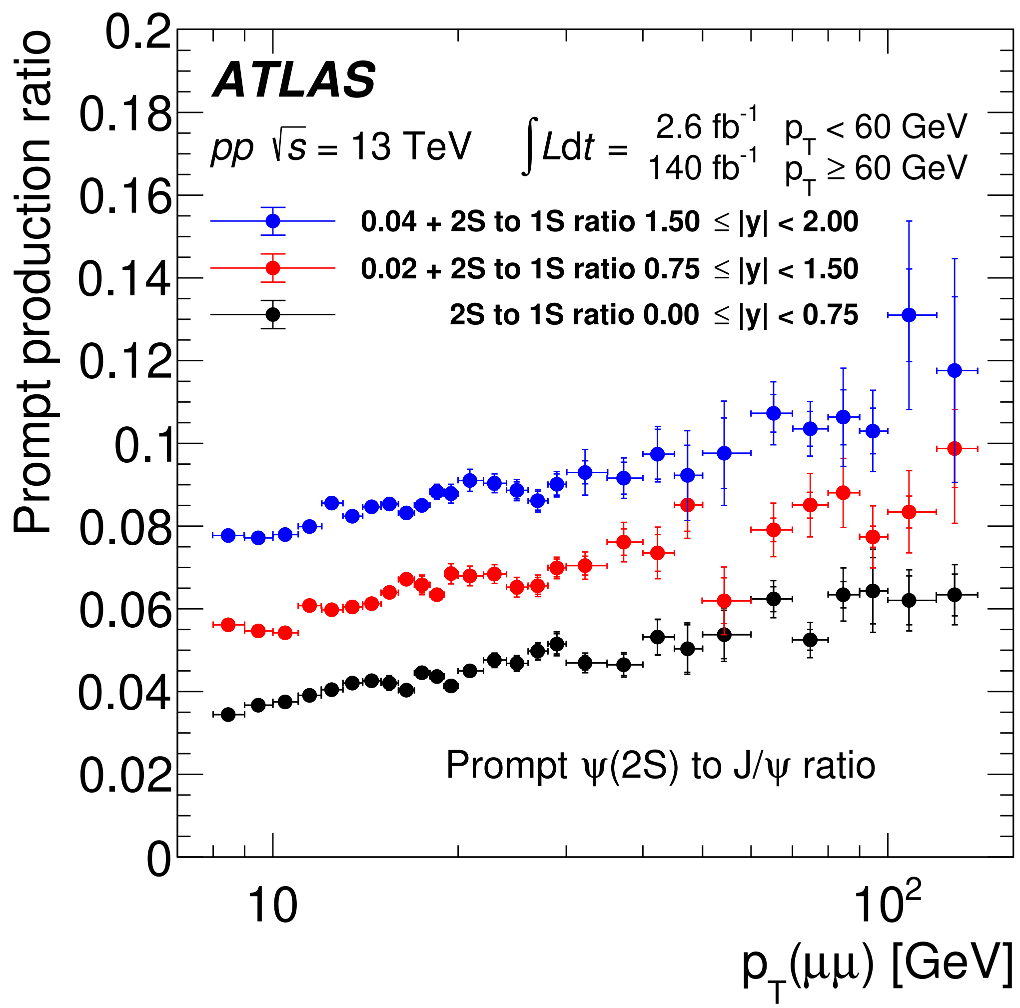

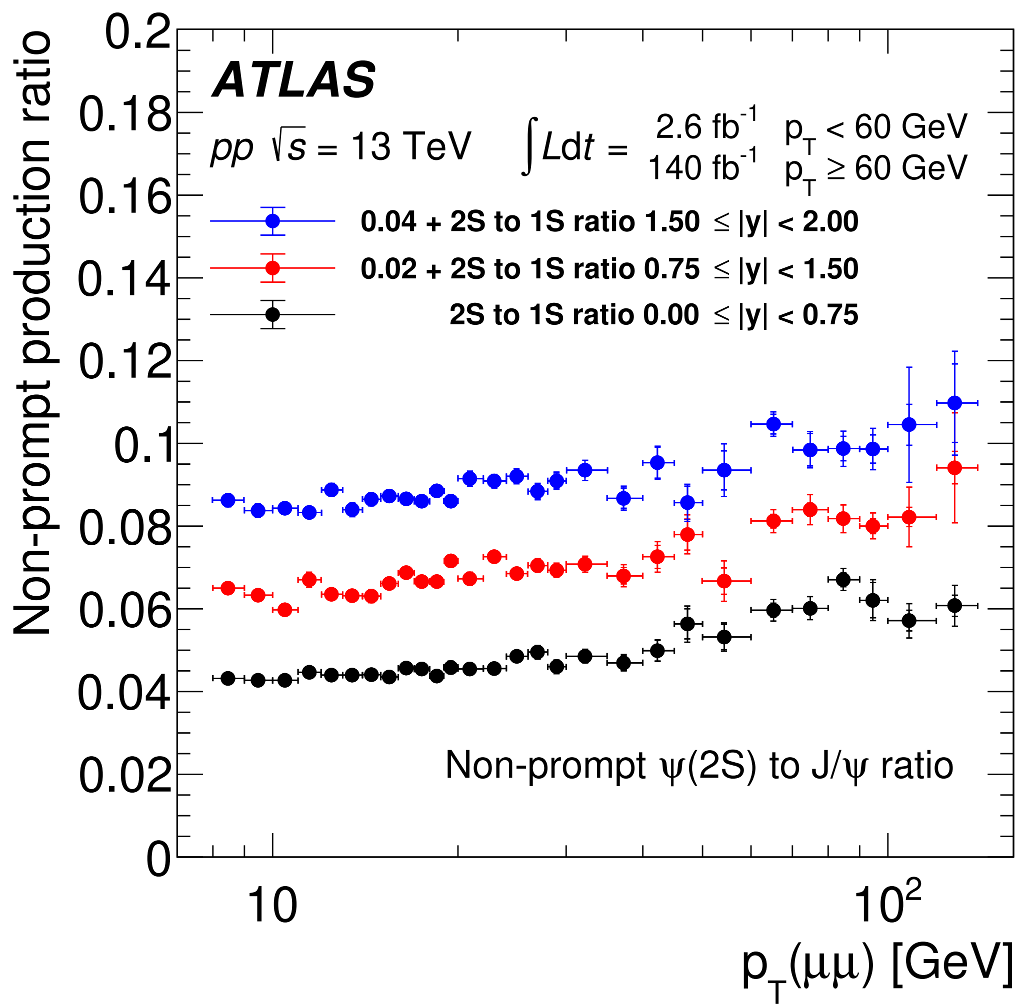

- The production ratios of $\psi(2S)$ relative to J/ψ for both prompt and non-prompt
  - Steadily increasing with increasing p_T
  - No obvius y dependence

Compare to theory prediction

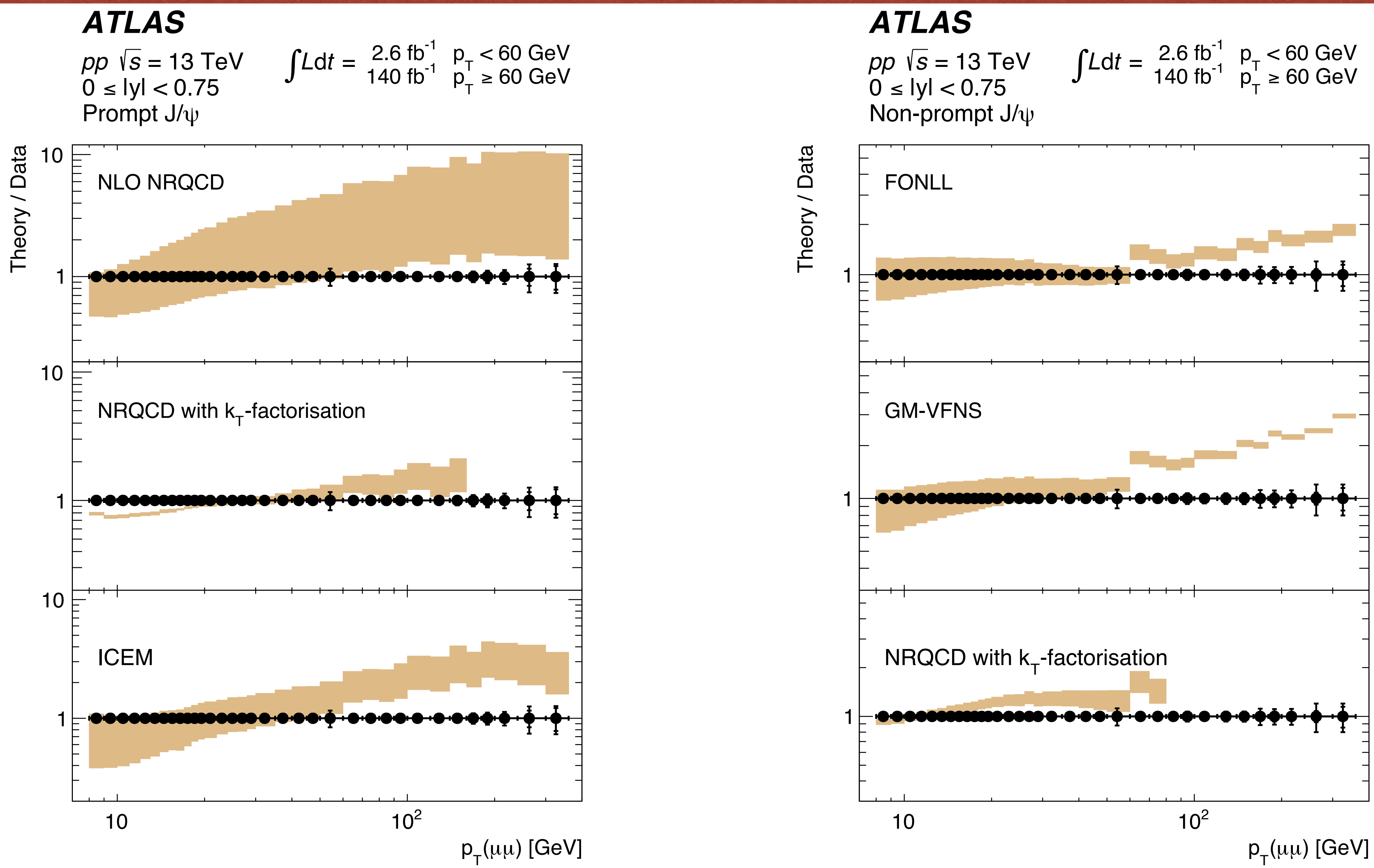

- Generally, all the considered models show a slower-than-observed decrease of cross section with p_T
  - Prompt: much harder p_T spectrum is predicted
  - Non-prompt: generally better at low p_T, but overestimate at high p_T

di-charmonium resonances

Phys. Rev. Lett. 131 (2023) 151902

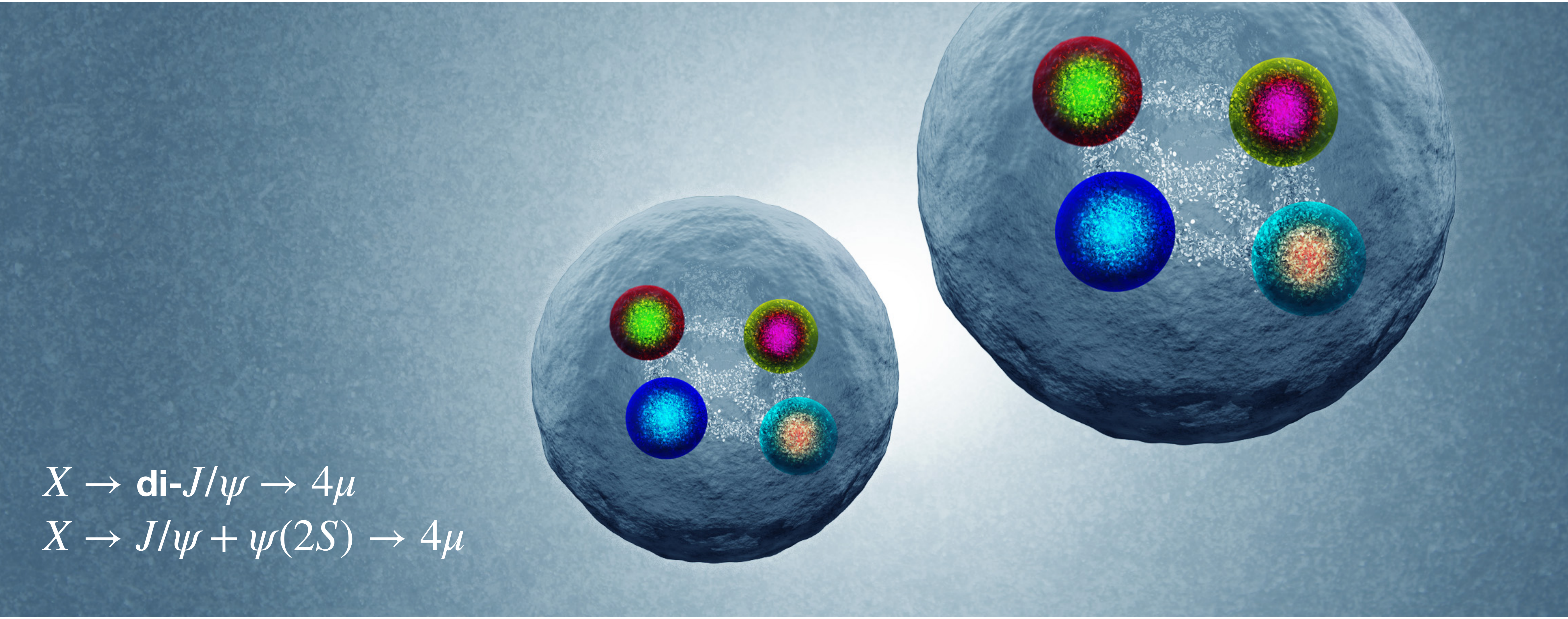

$X \rightarrow$ **di-**$J/\psi \rightarrow 4\mu$

$X \rightarrow J/\psi + \psi(2S) \rightarrow 4\mu$

Introduction

Charmonium ($c\bar{c}$) -like exotic hadrons

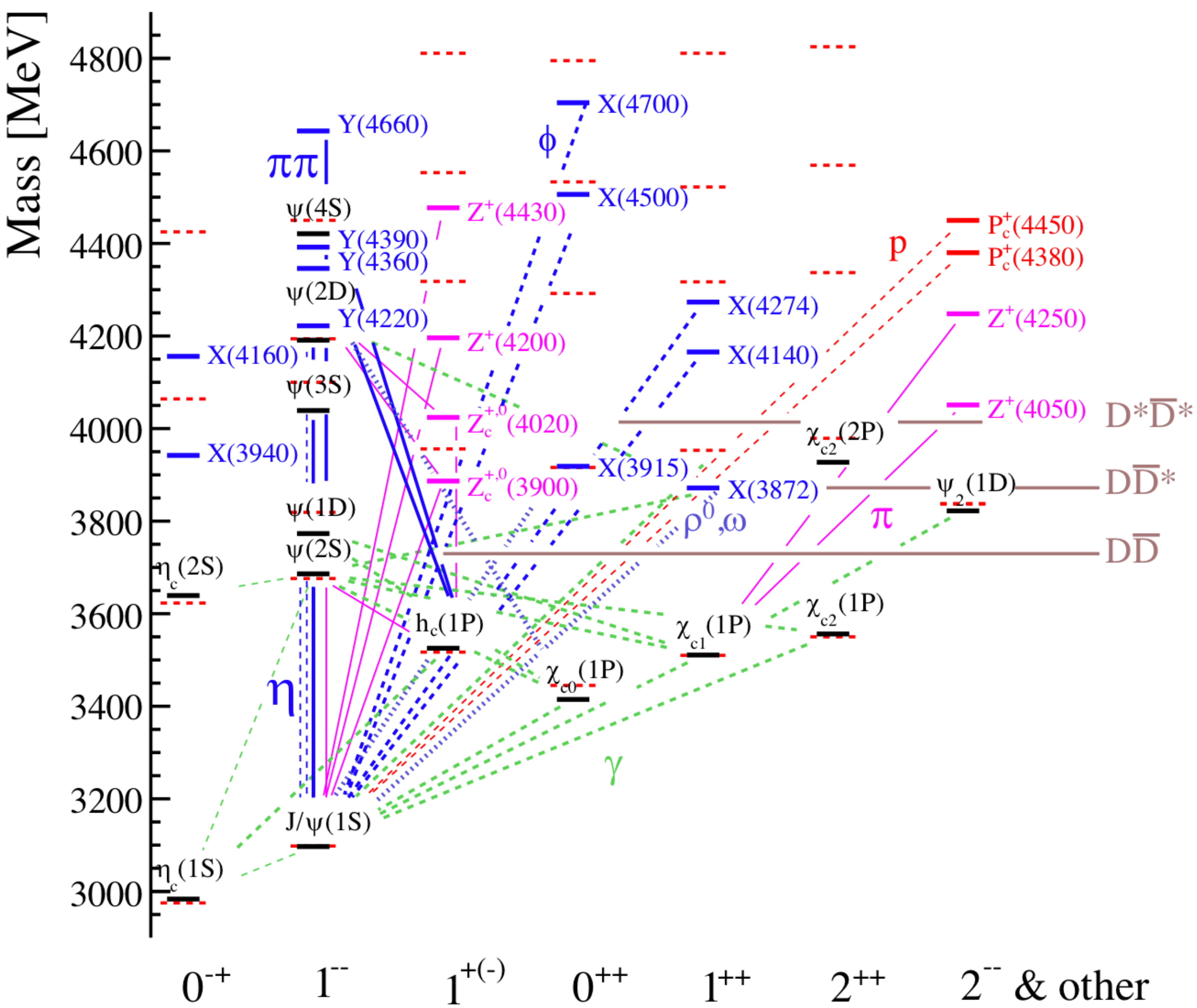

Rev. Mod. Phys. 90, 15003 (2018)

- A series of XYZ states was observed
- Lack observations of full-heavy tetraquarks which can make the theory-experiment comparison easier
  - First proposal of full-charm tetraquark (1975): Prog. of Theor. Phys., Vol 54, No. 2
  - The first calculation of the full-charm tetraquark mass (1981): Z. Phys. C 7 (1981) 317
  - First observation of potential full-charm tetraquark X(6900) (2020): LHCb Science Bulletin 65 (2020) 1983

XYZ states:

- X: neutral particle with $J^{PC} \neq 1^{--}$
- Y: neutral particle with $J^{PC} = 1^{--}$
- Z: charged particle

Signal process

- Tetraquark $(c\bar{c}c\bar{c}) \rightarrow J/\psi + J/\psi$ or $J/\psi + \psi(2S) \rightarrow 4\mu$

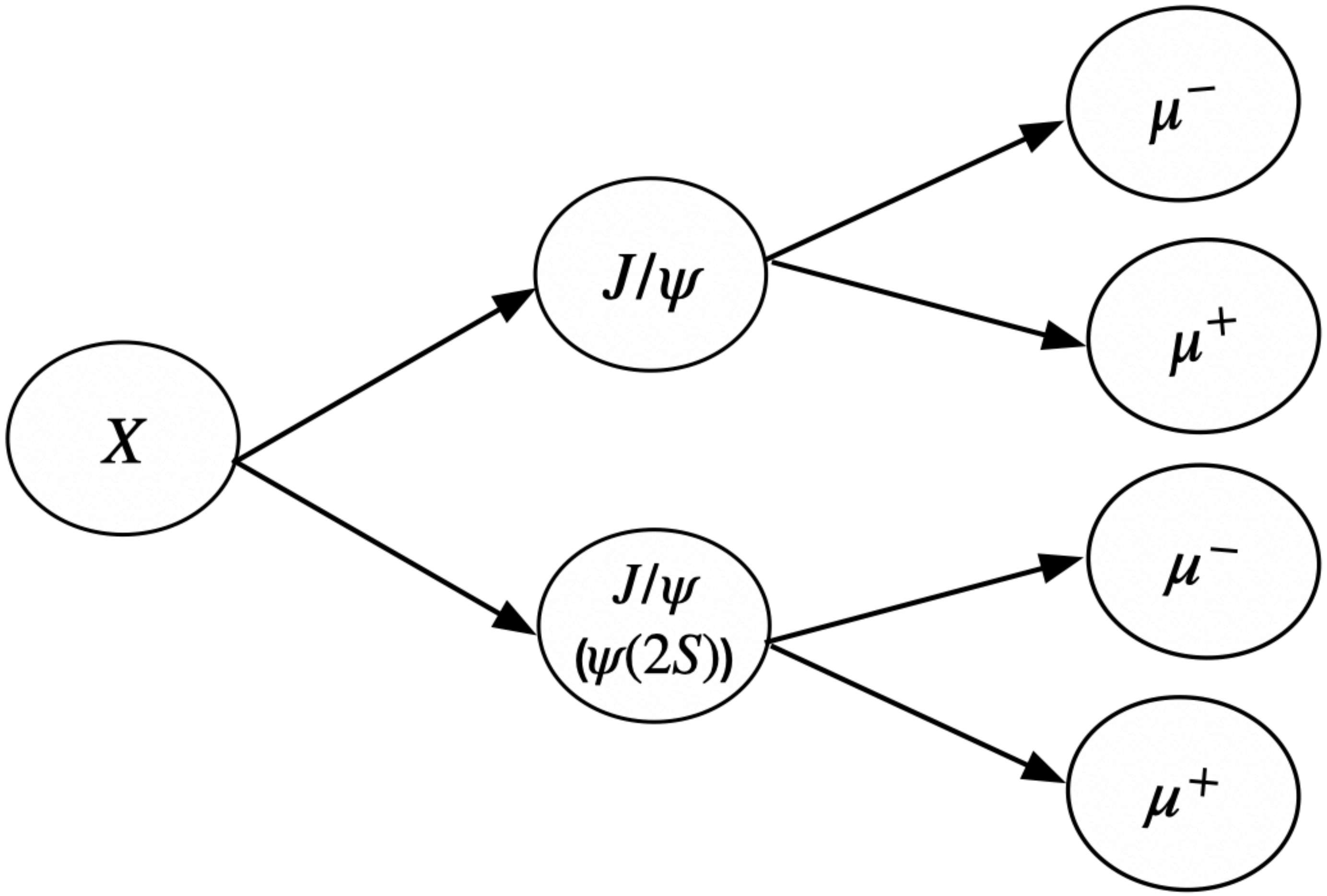

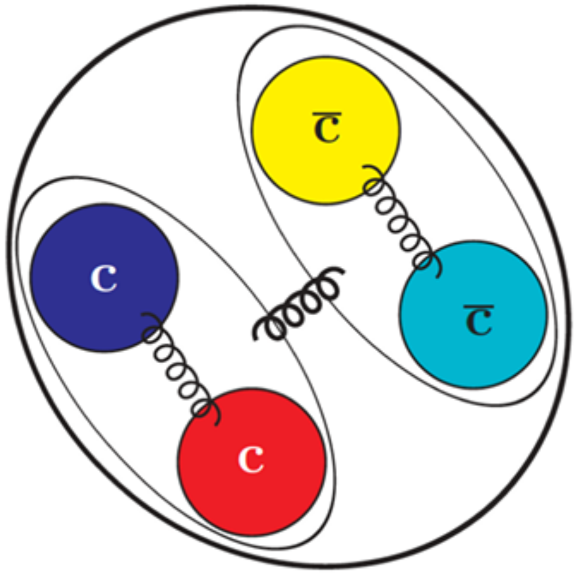

- How to reconstruct the 4μ candidate?
  - Find four muons with two opposite-charge pairs
  - Fit their inner detector tracks to a common vertex
  - Each pair is revertexed with a J/ψ or $\psi(2S)$ mass constraint

Signal process

- Tetraquark $(c\bar{c}c\bar{c}) \to J/\psi + J/\psi$ or $J/\psi + \psi(2S) \to 4\mu$

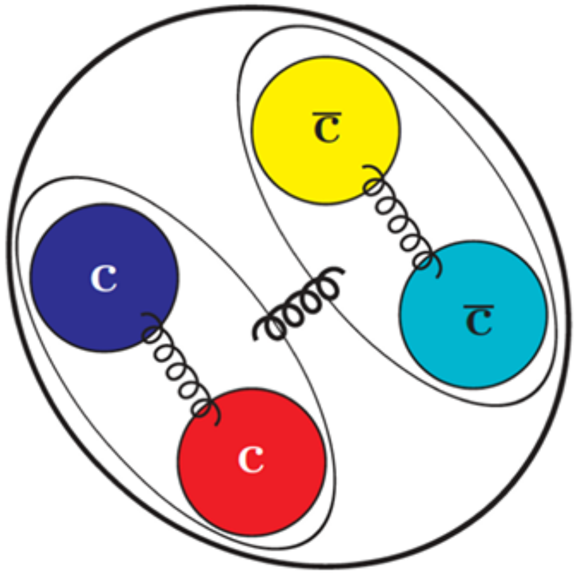

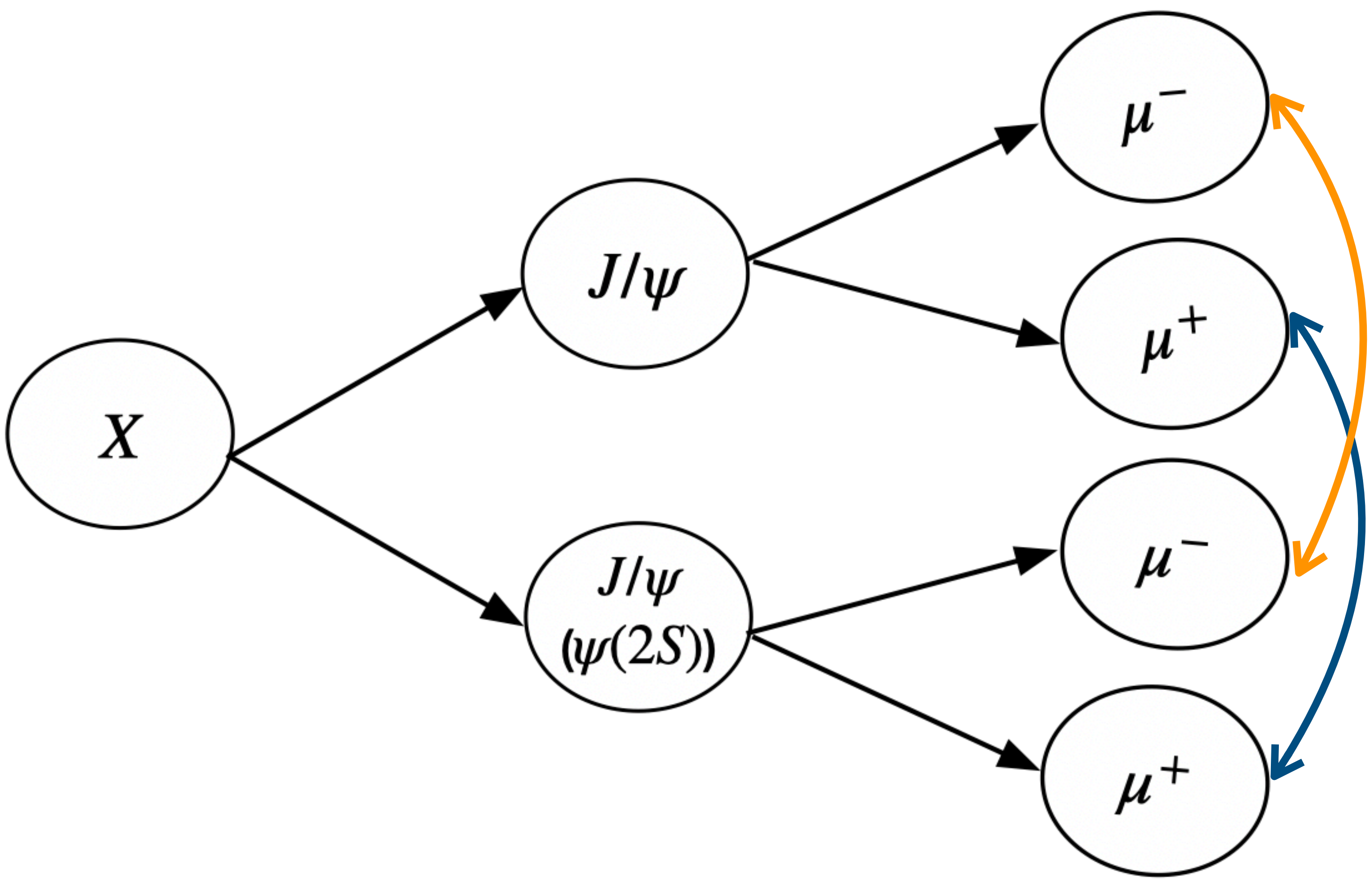

- How to reconstruct the 4μ candidate?
  - Find four muons with two opposite-charge pairs
  - Fit their inner detector tracks to a common vertex
  - Each pair is revertexed with a J/ψ or $\psi(2S)$ mass constraint

More than one candidate in the event?

The best candidate is chosen with $\sum \chi^2/N$ of the 4μ and di-muon vertices

Background sources

- Prompt backgrounds:
  - **Single parton scattering (SPS)**: a pair of ψ mesons can be produced in a single interaction
  - **Double parton scattering (DPS)**: a pair of ψ mesons can be produced in two separate interactions of gluons or quarks
- **Non-prompt** ($b\bar{b} \to J/\psi + J/\psi(\psi(2S)) \to 4\mu$)
- Single J/ψ background and non-peaking background containing no real J/ψ candidate (**Others**)
- In the di-J/ψ channel, the feed-down from $J/\psi + \psi(2S)$ channel to di-J/ψ channel is treated as an additional background

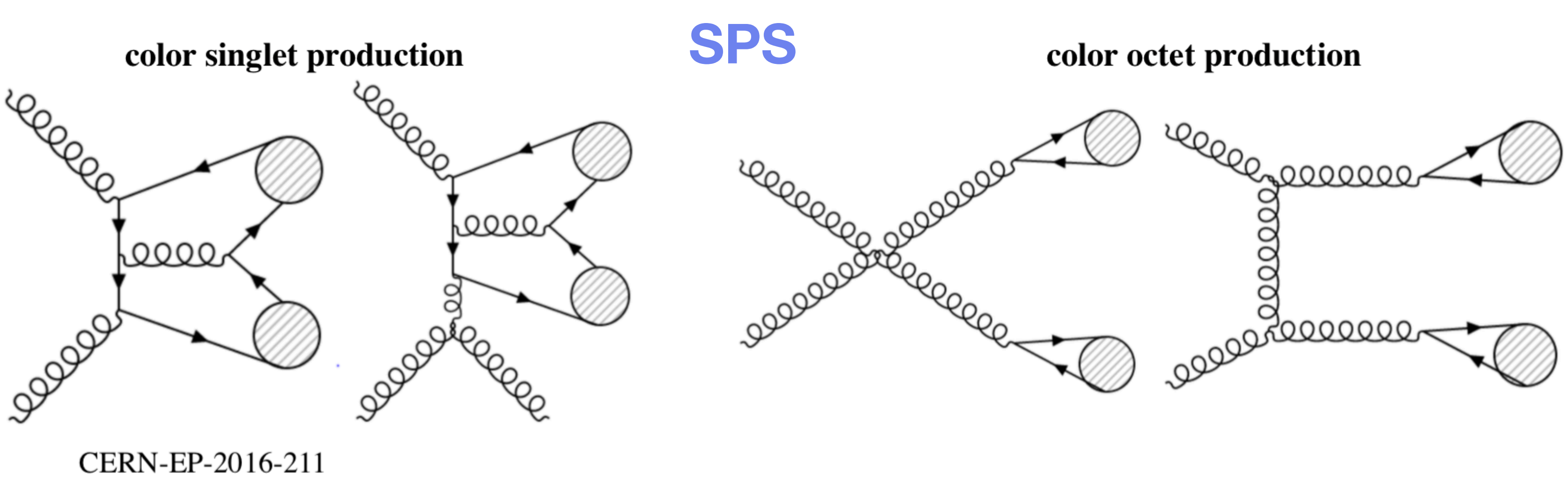

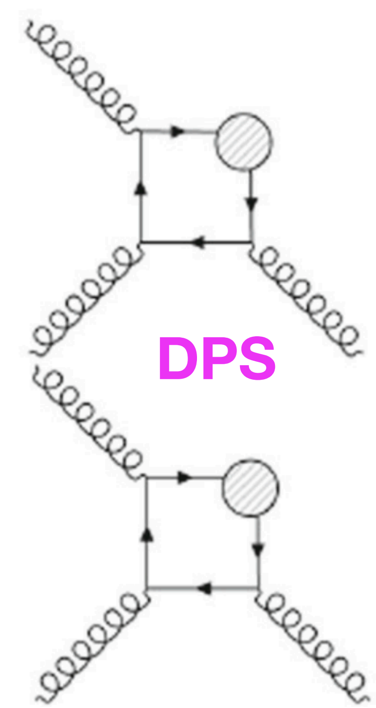

Event selections and analysis regions

- Baseline selections:
  - $p_T > 4,\ 4,\ 3,\ 3$ GeV and $|\eta| < 2.5$ for the four muons
  - J/ψ and $\psi(2S)$ mass requirement
  - Vertex fit quality (χ^2/N) and L_{xy} requirements

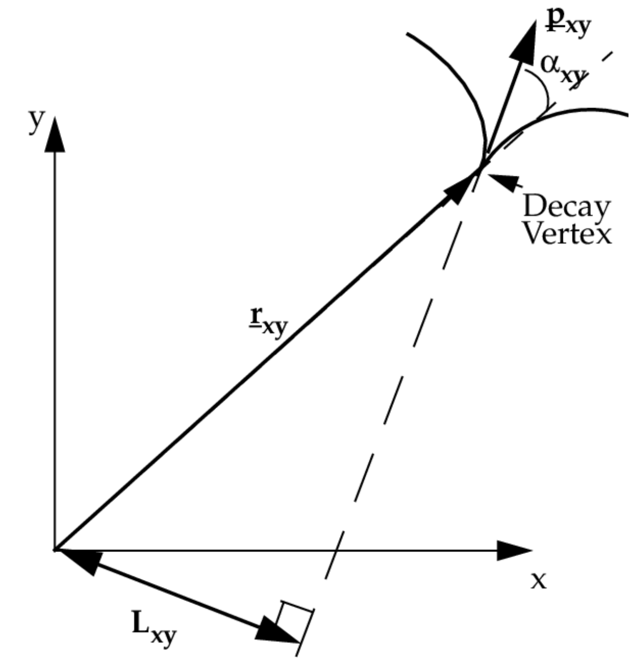

Reduce backgrounds without ψ mesons

Reduce non-prompt background

Signal	Vertex cuts: $\lvert L_{xy}^{di-\mu} \rvert < 0.3$ mm, $L_{xy}^{4\mu} < 0.2$ mm, $\chi^2_{4\mu}/N < 3$	$m_{4\mu} < 7.5$ GeV, $\Delta R < 0.25$ between charmonia
SPS		7.5 GeV $< m_{4\mu} < 12.0$ GeV
DPS		14.0 GeV $< m_{4\mu} < 25.0$ GeV
Non-prompt region	Reverse vertex cuts: $\chi^2_{4\mu}/N > 6$ and $\lvert L_{xy}^{di-\mu} \rvert > 0.4$ mm	

Feed-down background

- In the di-J/ψ channel, the feed-down from $J/\psi + \psi(2S)$ channel to di-J/ψ channel is treated as an additional background

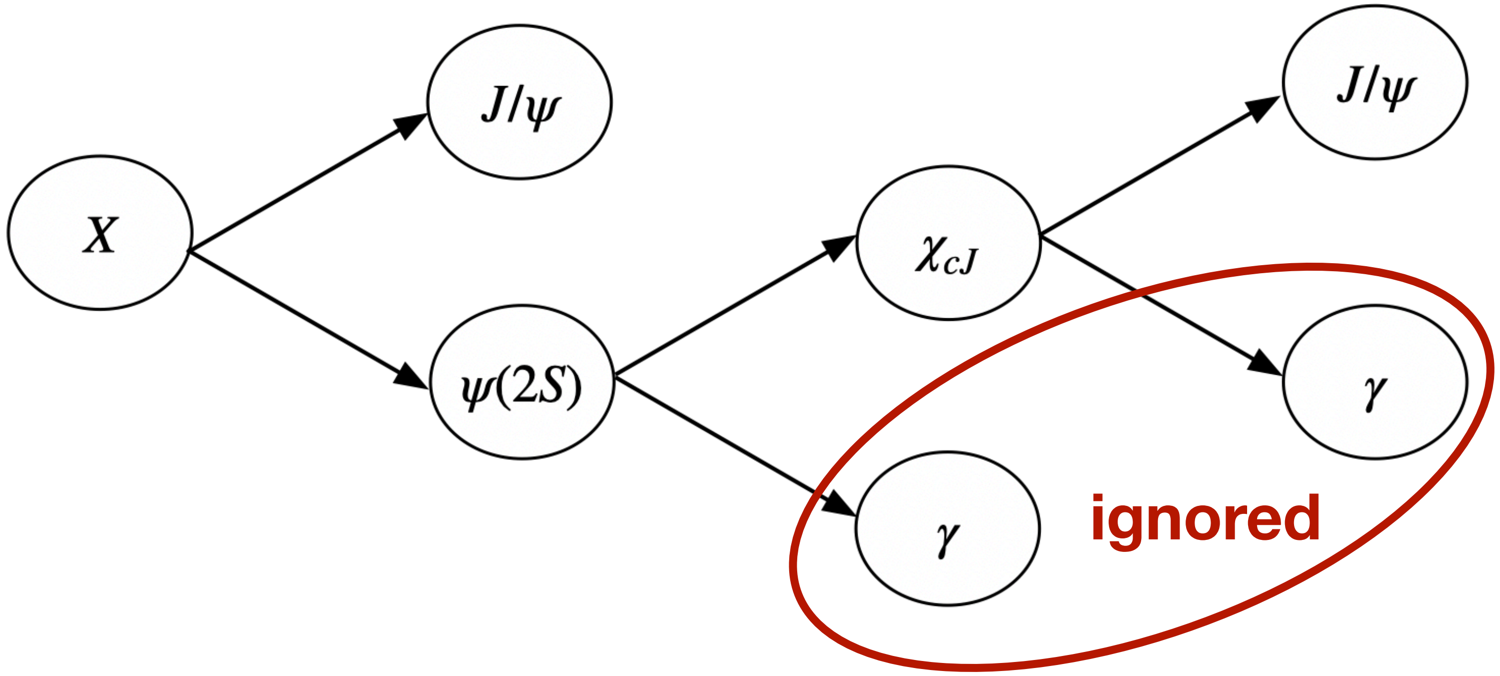

- The normalisation is extracted with the fitted signal yields in the $J/\psi + \psi(2S)$ channel

$$N_{\text{fd}} = \frac{\mathcal{B}' \epsilon'}{\mathcal{B}\left(\psi(2S) \to \mu\mu\right) \epsilon} N$$

Feed-down background

- In the di-J/ψ channel, the feed-down from $J/\psi + \psi(2S)$ channel to di-J/ψ channel is treated as an additional background

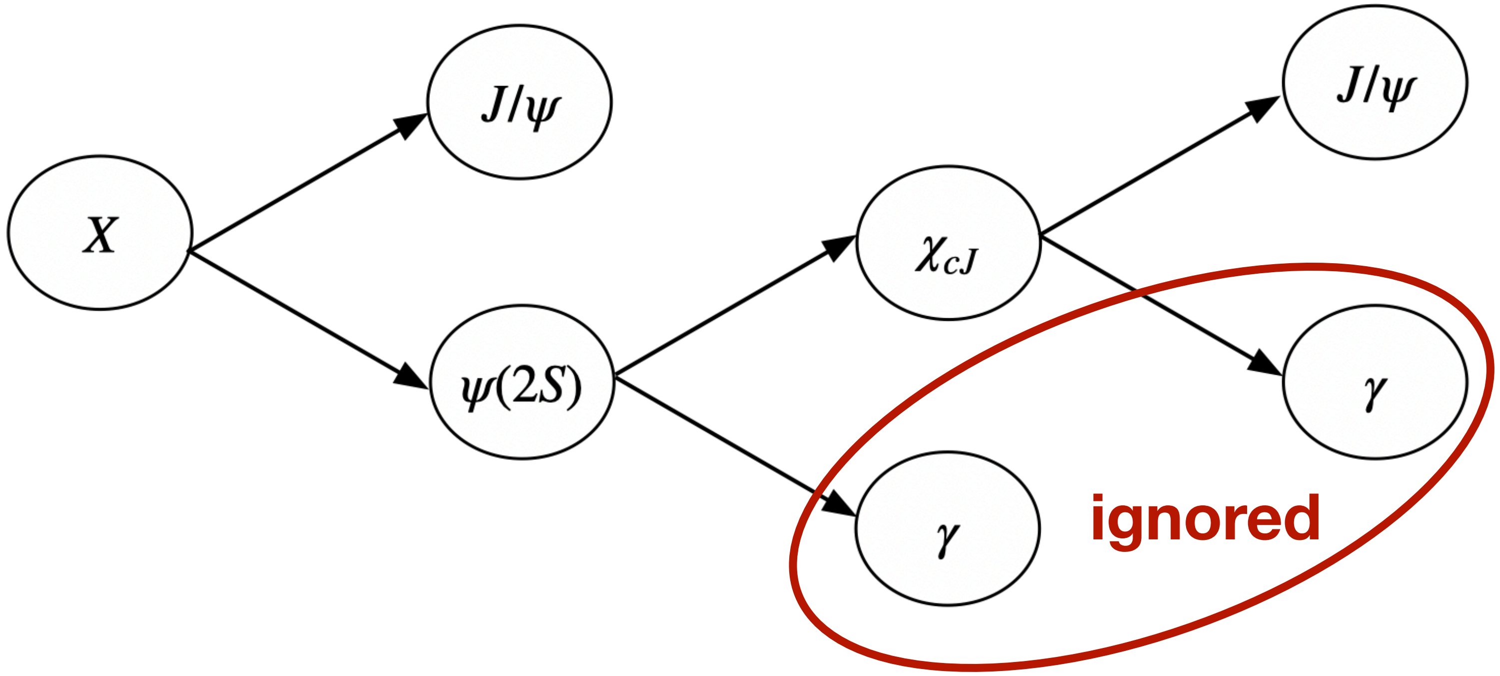

- The normalisation is extracted with the fitted signal yields in the $J/\psi + \psi(2S)$ channel

$$N_{\rm fd} = \frac{\mathcal{B}'\epsilon'}{\mathcal{B}\left(\psi(2S) \to \mu\mu\right)\epsilon} N$$

signal eff. in $J/\psi + \psi(2S)$

feed-down eff. in di-J/ψ

$$\left[\mathcal{B}\left(\psi(2S) \to J/\psi + X\right) + \mathcal{B}\left(\psi(2S) \to \gamma\chi_{cJ}\right)\mathcal{B}(\chi_{cJ} \to \gamma J/\psi)\right]\mathcal{B}(J/\psi \to \mu\mu)$$

$X: \pi^+\pi^-, \pi^0\pi^0, \eta, \pi^0$

Fit models

- Unbinned maximum likelihood fits are performed to extract the signal parameters (e.g. mass m, width Γ)

$$\mathcal{L} = \mathcal{L}_{SR}\left(\vec{\theta}, \vec{\lambda}\right) \cdot \mathcal{L}_{CR}\left(\vec{\theta}\right) \cdot \prod_{j=1}^{K} G\left(\theta'_j; \theta_j, \sigma_j\right)$$

- Fit regions:
  - Fit SR: $m_{4\mu} < 11$ GeV and $\Delta R < 0.25$
  - Fit CR: $m_{4\mu} < 11$ GeV and $\Delta R \geq 0.25$

- Only systematics affecting the mass spectrum shape are included (backup)

Fit regions in di-J/ψ channel

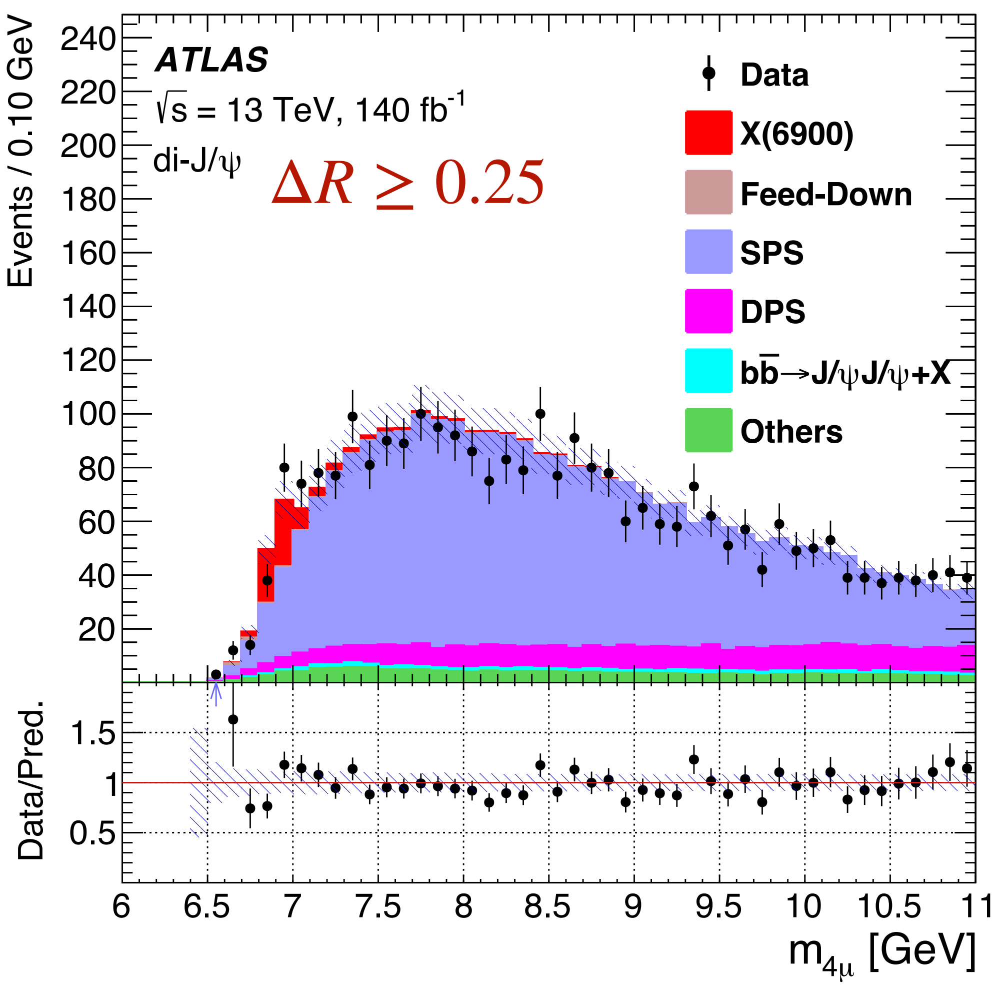

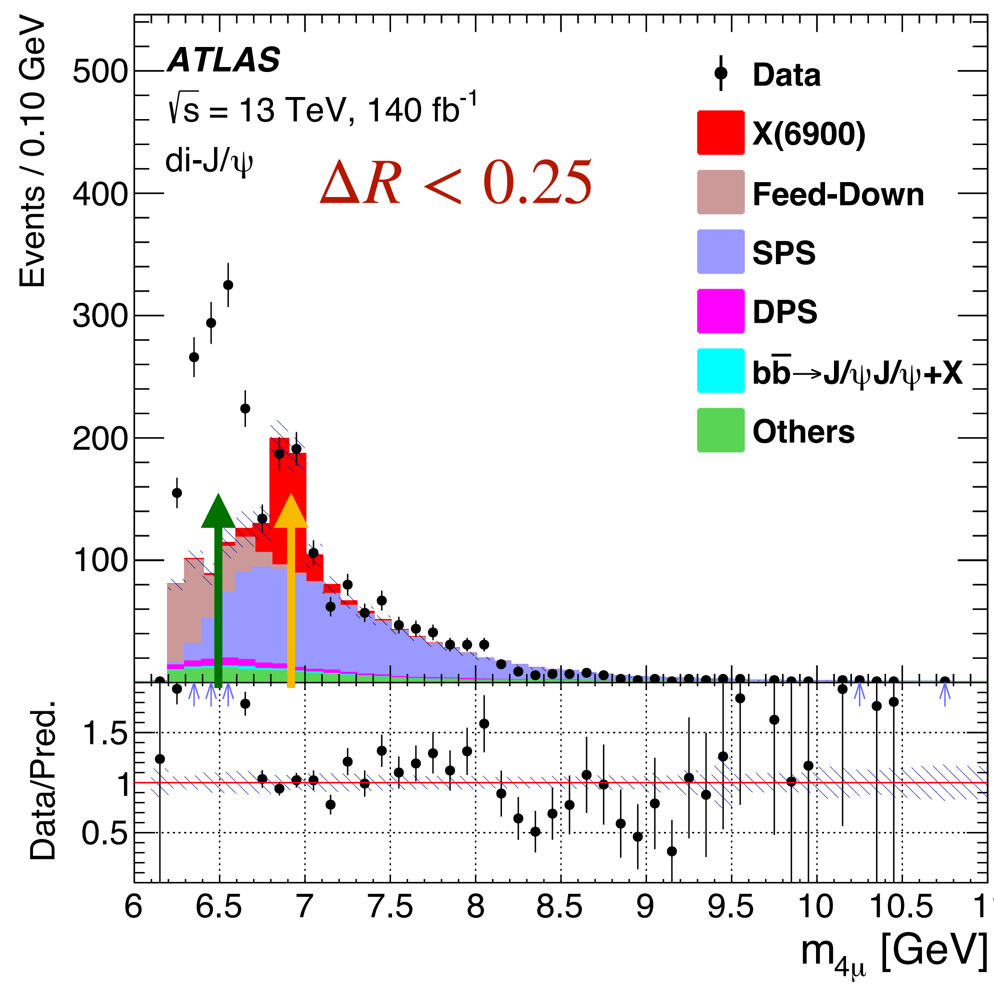

- SPS mass shape is modelled well

- A broad structure near threshold from **6.2 to 6.8 GeV**
- A narrow structure around **6.9 GeV**

Fit regions in $J/\psi + \psi(2S)$ channel

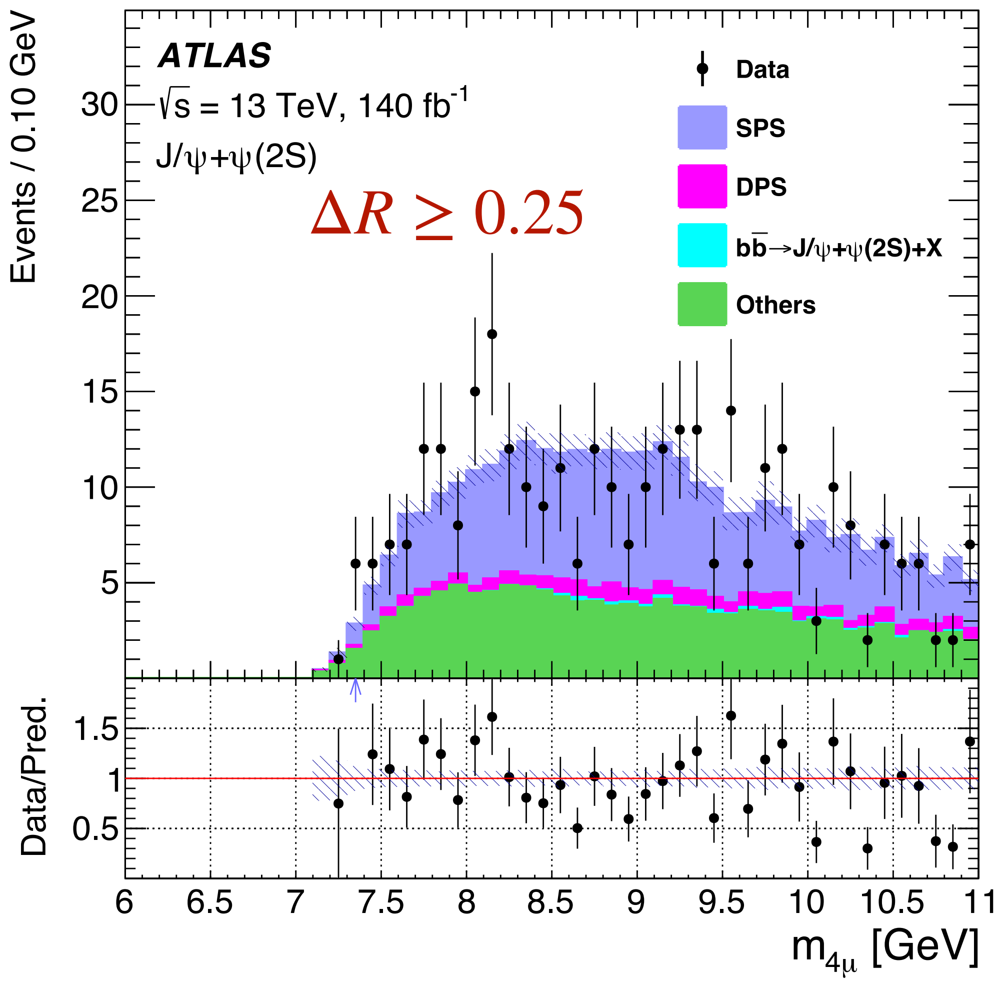

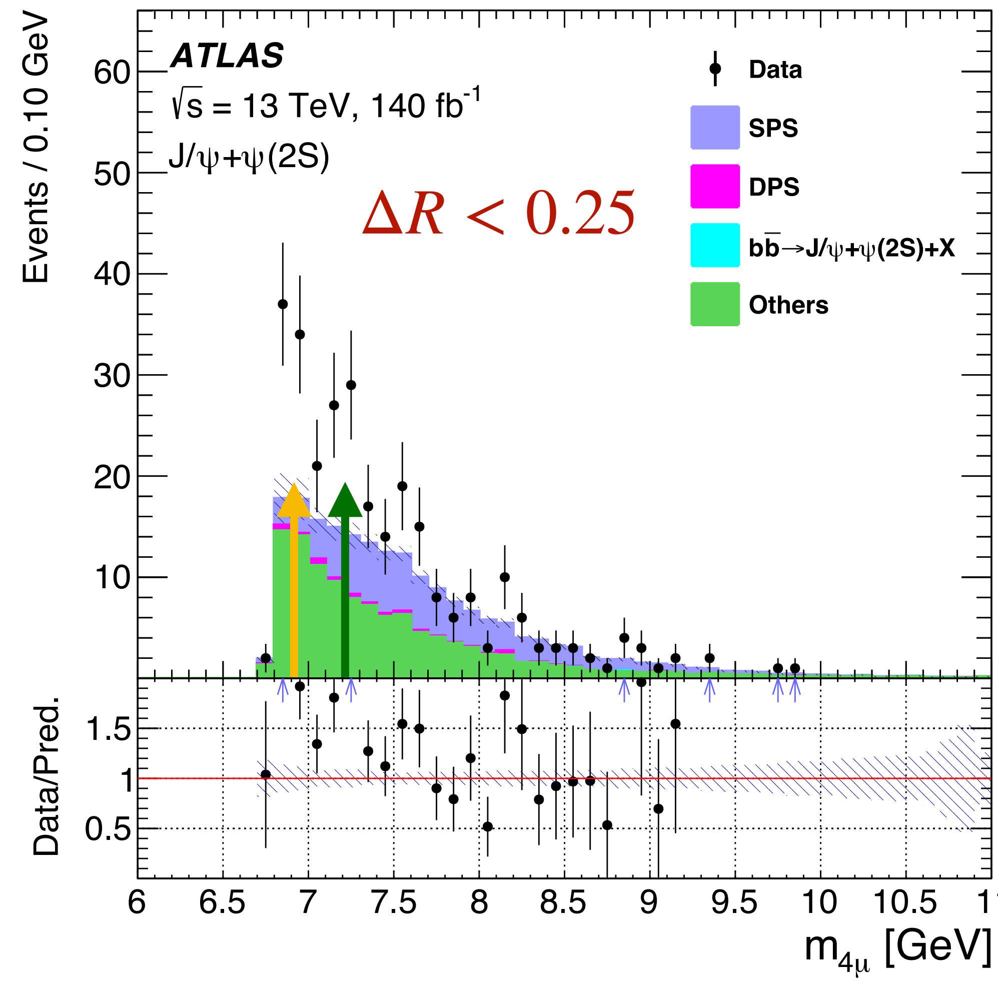

- SPS mass shape is modelled well

- A narrow structure around **6.9 GeV**
- Hint for another narrow structure around **7.2 GeV**

Signal model

- The di-J/ψ channel:
  - Model A: **3-peak signal model** with interference among signals

$$f_s(x) = \left| \sum_{i=0}^{2} \frac{z_i}{m_i^2 - x^2 - i m_i \Gamma_i(x)} \right|^2 \sqrt{1 - \frac{4m_{J/\psi}^2}{x^2}} \otimes R(\theta)$$

  - Model B: 2-peak model with the first one interfering with the SPS background plus a standalone peak

$$f(x) = \left(\left| \frac{z_0}{m_0^2 - x^2 - i m_0 \Gamma_0(x)} + A(x) e^{i\phi} \right|^2 + \left| \frac{z_2}{m_2^2 - x^2 - i m_2 \Gamma_2(x)} \right|^2 \right) \sqrt{1 - \frac{4m_{J/\psi}^2}{x^2}} \otimes R(\theta)$$

Resolution function

phase space factor

Signal model

- The $J/\psi + \psi(2S)$ channel:
  - Model α: the same peaks with interference observed in the di-J/ψ channel also decaying into $J/\psi + \psi(2S)$ plus a standalone peak

$$f_s(x) = \left(\left| \sum_{i=0}^{2} \frac{z_i}{m_i^2 - x^2 - i m_i \Gamma_i(x)} \right|^2 + \left| \frac{z_3}{m_3^2 - x^2 - i m_3 \Gamma_3(x)} \right|^2 \right) \sqrt{1 - \left(\frac{m_{J/\psi} + m_{\psi(2S)}}{x} \right)^2} \otimes R(\theta)$$

  - Model β: only one single peak

Fit results in di-J/ψ channel

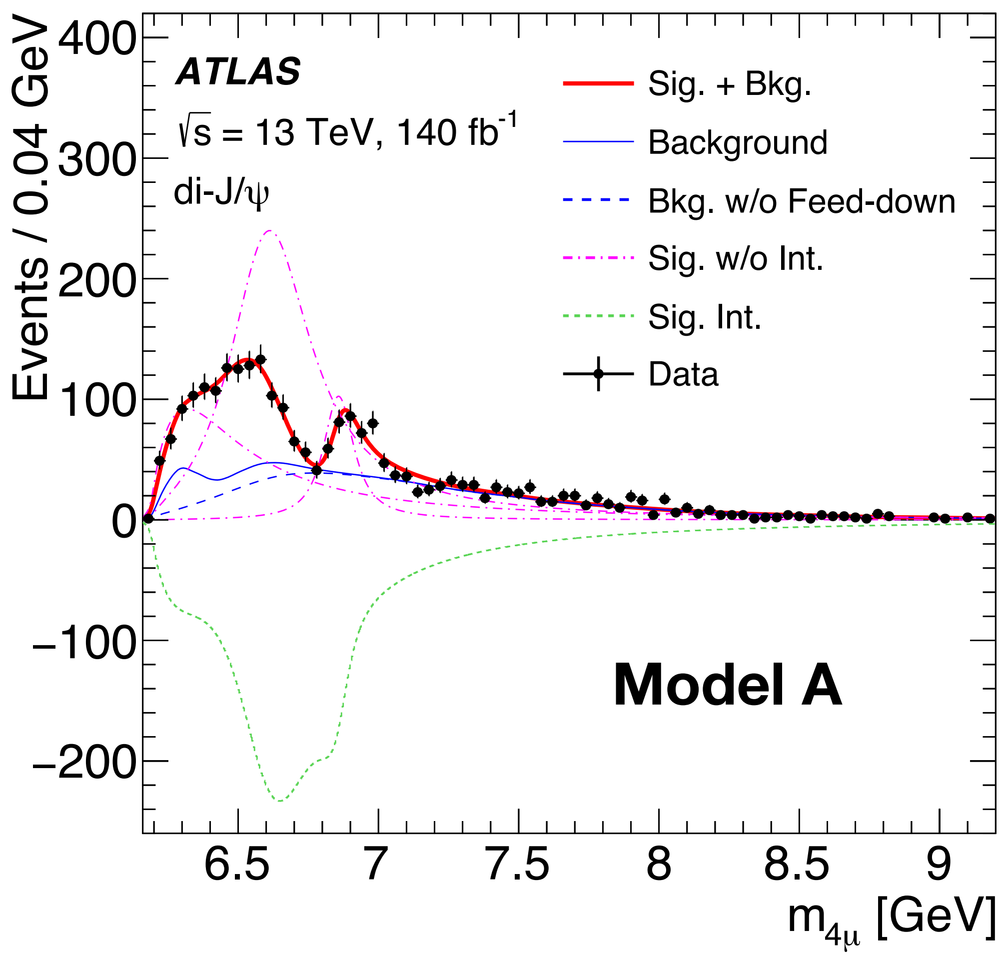

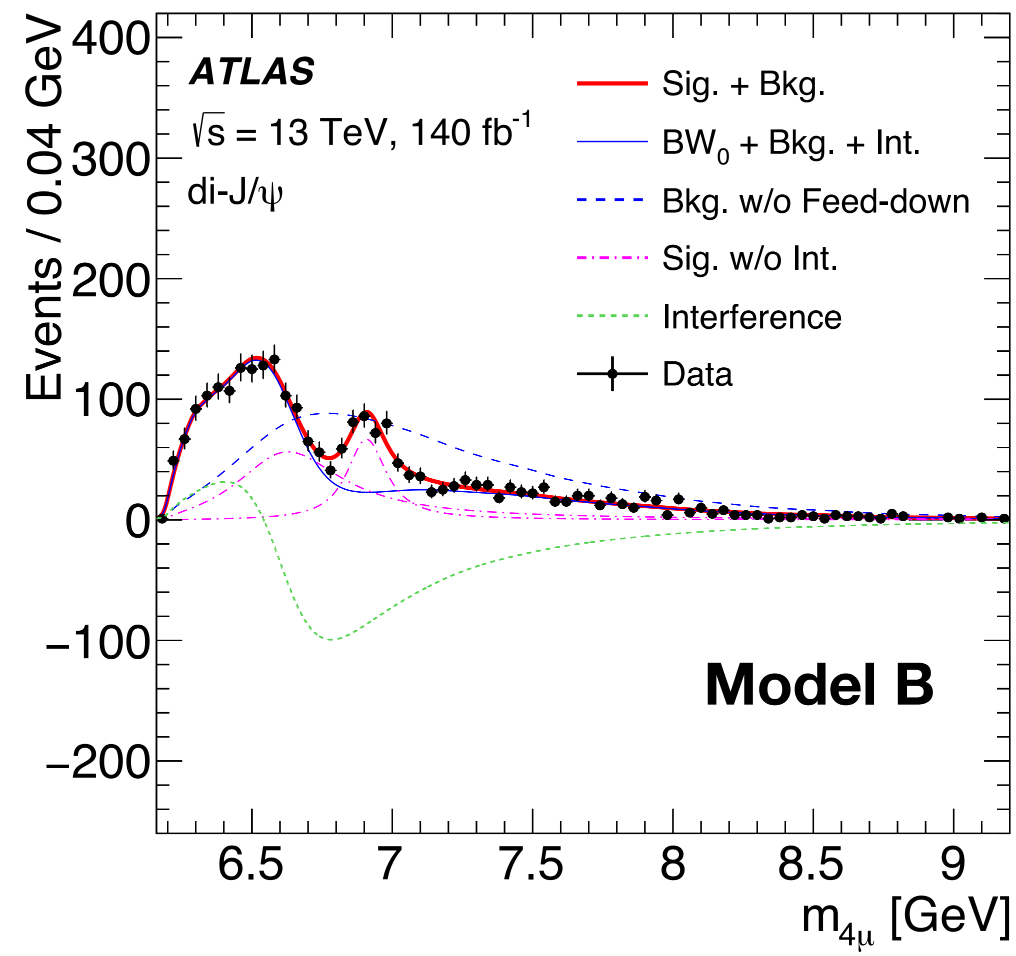

- Two signal models are tested:
  - **Model A**: three interfering signal peaks
  - **Model B**: two signal peaks
- The peak around **6.9 GeV** is consistent with the LHCb observed X(6900) (Science Bulletin 65 (2020) 1983), with significance far above 5σ

di-J/ψ	model A	model B
m_0	$6.41 \pm 0.08^{+0.08}_{-0.03}$	$6.65 \pm 0.02^{+0.03}_{-0.02}$
Γ_0	$0.59 \pm 0.35^{+0.12}_{-0.20}$	$0.44 \pm 0.05^{+0.06}_{-0.05}$
m_1	$6.63 \pm 0.05^{+0.08}_{-0.01}$	—
Γ_1	$0.35 \pm 0.11^{+0.11}_{-0.04}$	
m_2	$6.86 \pm 0.03^{+0.01}_{-0.02}$	$6.91 \pm 0.01 \pm 0.01$
Γ_2	$0.11 \pm 0.05^{+0.02}_{-0.01}$	$0.15 \pm 0.03 \pm 0.01$
$\Delta s/s$	$\pm 5.1\%^{+8.1\%}_{-8.9\%}$	—

Fit results in $J/\psi + \psi(2S)$ channel

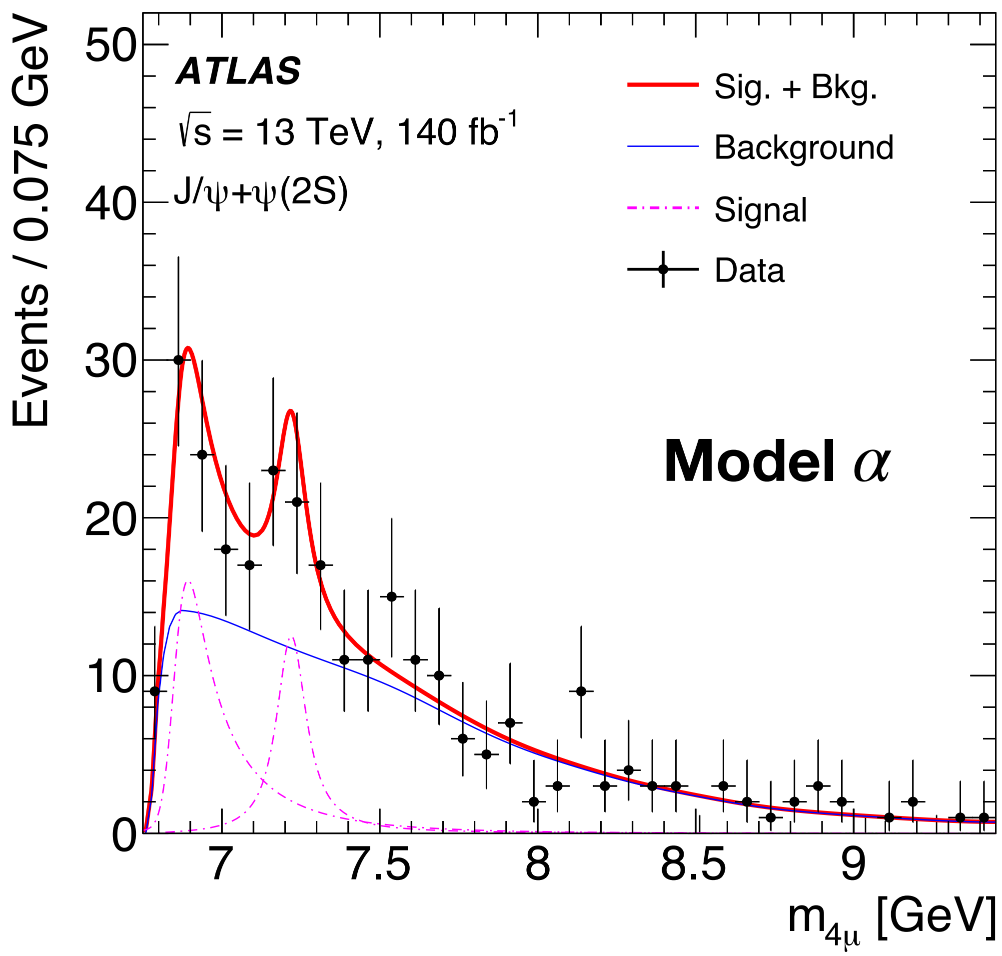

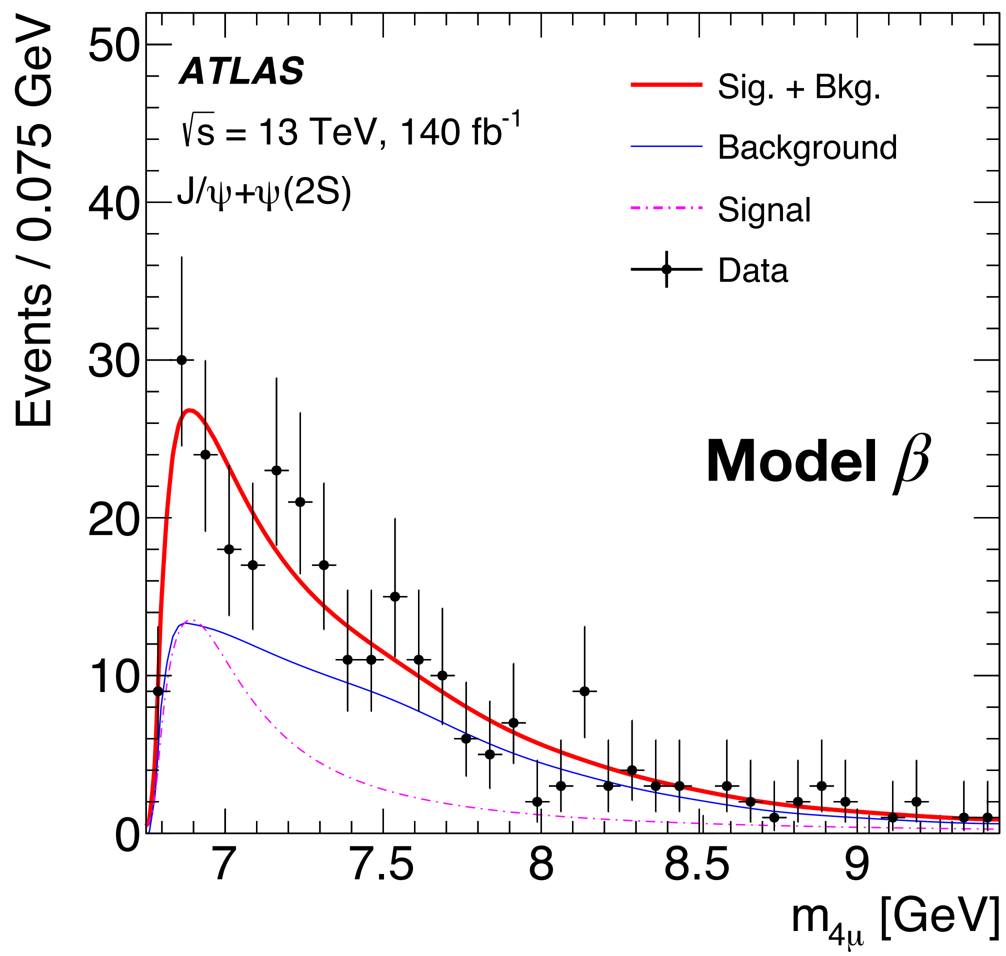

- Two signal models are tested:
  - **Model** α: the same peaks observed in the di-J/ψ channel also decaying into $J/\psi + \psi(2S)$ plus a standalone peak.
  - **Model** β: only one signal peak

J/ψ+ψ(2S)	model α	model β
m_3	$7.22 \pm 0.03^{+0.01}_{-0.04}$	$6.96 \pm 0.05 \pm 0.03$
Γ_3	$0.09 \pm 0.06^{+0.06}_{-0.05}$	$0.51 \pm 0.17^{+0.11}_{-0.10}$
$\Delta s/s$	$\pm 21\%^{+25\%}_{-15\%}$	$\pm 20\% \pm 12\%$

- The signal significance is 4.7σ (4.3σ) for model α (β). The significance of the **2nd peak** (7.2 GeV) reaches **3.0σ**, also hinted by LHCb and CMS (Phys.Rev.Lett. 132 (2024) 11, 111901) in the di-J/ψ spectrum

Summary

- Recent results in heavy flavour physics by ATLAS with full Run 2 data are presented:
  - $B^0 \rightarrow J/\psi K^{*0}$ lifetime measurement
  - Measurement of J/ψ and $\psi(2S)$ differential cross-section
  - Search for di-charmonium excesses in four-muon final state
- Cover a broad spectrum of the most interesting topics
- New measurements with the Run 2 and Run 3 data are on-going: stay tuned!

Thanks

The ATLAS Pixel detector

Barrel and Disk

- Three barrel layers, radii 50.5, 88.5, 122.5 mm
  - Innermost layer known as B-Layer
  - Active area: $1.45m^2$
  - Readout channels: 67M
- Three end-cap disks (per side)
  - Active area: $0.28m^2$
  - Readout channels: 13M
- Operating since 2008

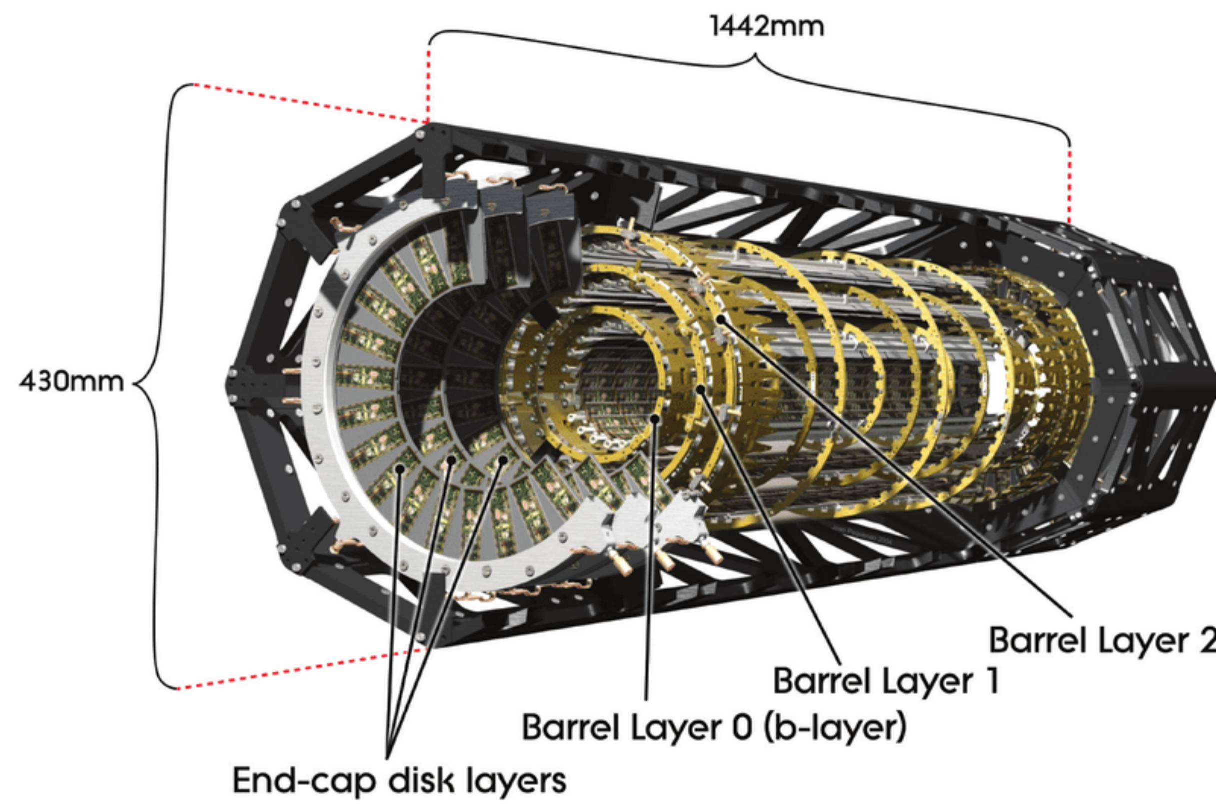

Module

- 16 FE-I3 chips with 250nm CMOS + 1 Module Control Chip
- 1 Planar n-in-n sensor, $250\mu m$ thick
- Radiation hard: 50 Mrad, ~$1 \times 10^{15} n_{\text{eq}}$ cm^{-2}

The insertable B-Layer

- Insertable B-Layer (IBL) was inserted during the first long LHC shutdown (2013-2014),
  - 14 staves, each at radius 33.5mm
  - Active area: $0.15m^2$
  - Readout channels: 12M
- Operating since 2015
- Five times better rejection of b-tagging than Run 1

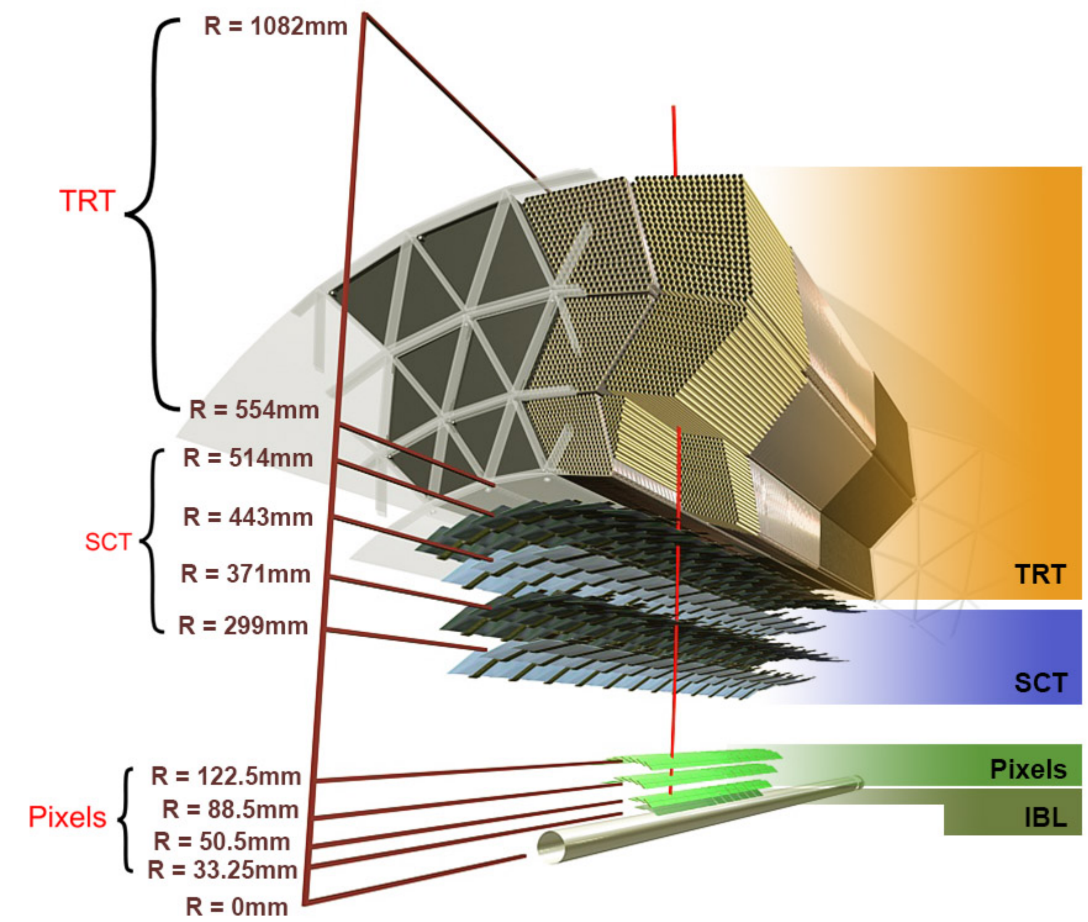

Module

- FE-I4 in 130 nm CMOS
- $200\mu m$ thick for planar sensor and $230\mu m$ for 3D sensors
- Radiation hard: 250 Mrad, $\sim 2 \times 10^{15} n_{\text{eq}}$ cm^{-2}

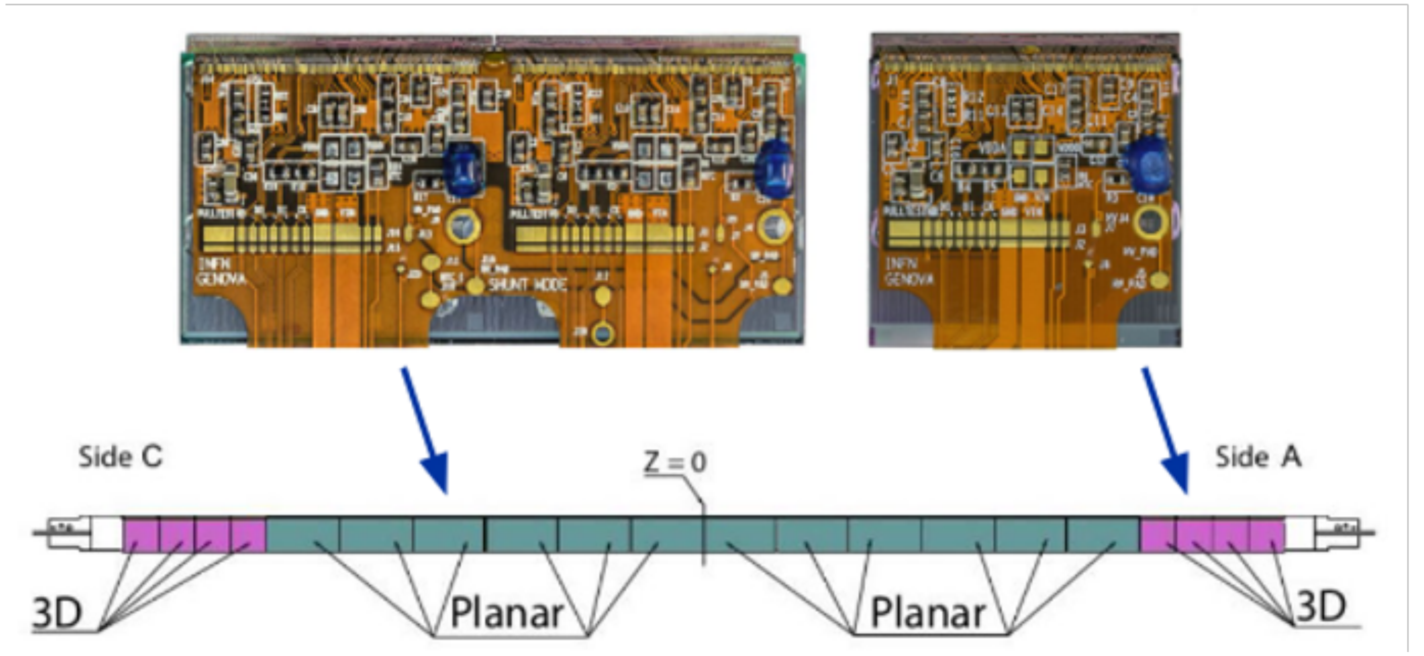

B^0 meson lifetime measurement: PDFs

- Mass PDFs
  - Signal: Johnson S_U-distribution

$$\mathcal{M}_{\text{sig}}(m_i) = \frac{\delta}{\lambda\sqrt{2\pi}\sqrt{1+\left(\frac{m_i-\mu}{\lambda}\right)^2}} \exp\left[-\frac{1}{2}\left(\gamma + \delta \sinh^{-1}\left(\frac{m_i-\mu}{\lambda}\right)\right)^2\right]$$

  - Background: polynomial + sigmoid function

$$\mathcal{M}_{\text{bkg}}(m_i) = f_{\text{poly}}(1 + p_0 \cdot m_i) + (1 - f_{\text{poly}})\left(1 - \frac{s(m_i - m_0)}{\sqrt{1 + (s(m_i - m_0))^2}}\right)$$

- Proper decay time PDFs (resolution functions applied)
  - Signal: exponential function

$$R(t' - t_i, \sigma_{t_i}) = \sum_{k=1}^{3} f_{\text{res}}^{(k)} \frac{1}{\sqrt{2\pi}\, S^{(k)}\, \sigma_{t_i}} \exp\left(\frac{-(t' - t_i)^2}{2(S^{(k)}\, \sigma_{t_i})^2}\right)$$

$$P_{\text{sig}}(t_i|\sigma_{t_i}, p_{\text{T}_i}) = E(t', \tau_{B^0}) \otimes R(t' - t_i, \sigma_{t_i})$$

$$E(t, \tau_{B^0}) = (1/\tau_{B^0}) \exp(-t/\tau_{B^0}) \text{ for } t \geq 0$$

  - Background:

$$P_{\text{bkg}}(t_i|\sigma_{t_i}, p_{\text{T}_i}) = \left(f_{\text{prompt}} \cdot \delta_{\text{Dirac}}(t') + (1 - f_{\text{prompt}}) \sum_{k=1}^{3} b_k \prod_{l=1}^{k-1} (1 - b_l) E(t', \tau_{\text{bkg}_k})\right) \otimes R(t' - t_i, \sigma_{t_i})$$

Cross-section measurement of J/ψ and $\psi(2S)$ mesons: PDFs

- Mass
  - J/ψ ($\psi(2S)$): Gaussian and Crystal Ball
  - Prompt background: Bernstein polynomials
  - Non-prompt background: Exponential

Cross-section measurement of J/ψ and $\psi(2S)$ mesons

- Spin alignment corrections. Here only show J/ψ differential cross-section and non-prompt production fraction. But were found to be essentially the same for J/ψ and $\psi(2S)$, for the prompt and non-prompt production mechanisms, and also for the three rapidity regions
- Potential bias due to the spin-alignment assumption at 60GeV causes a step in the J/ψ non-prompt production at the same point

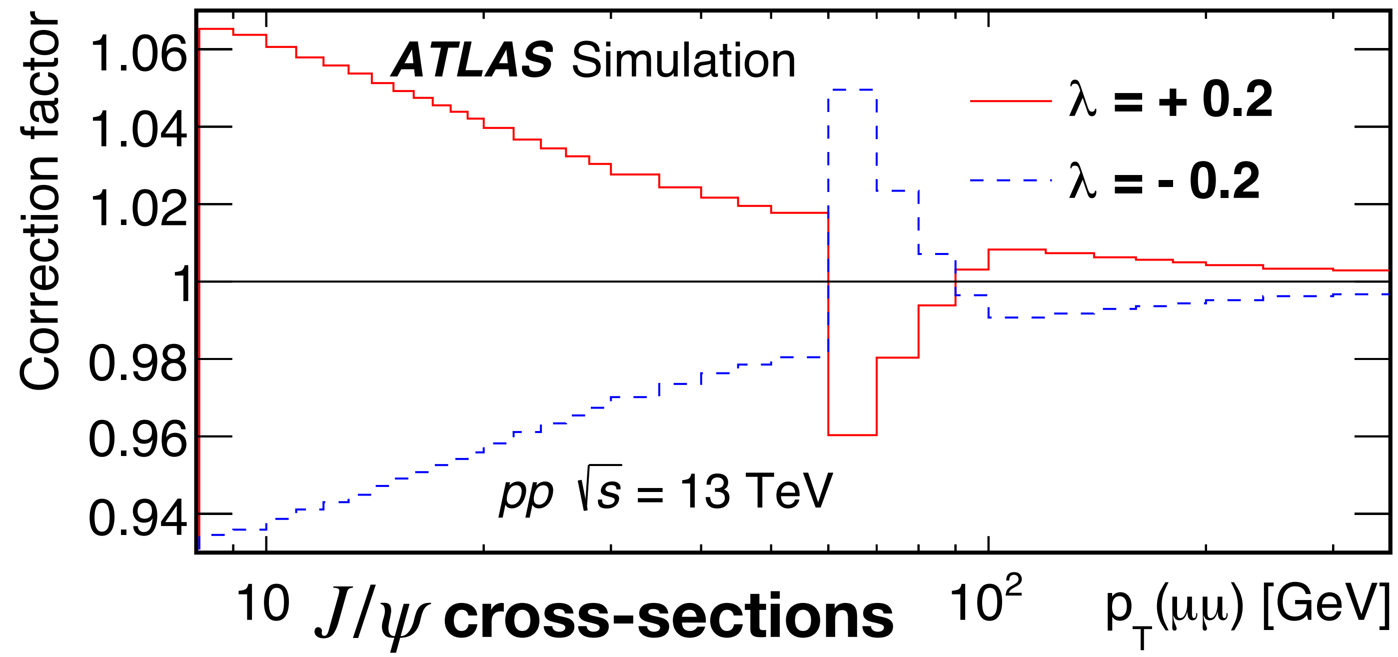

J/ψ cross-sections

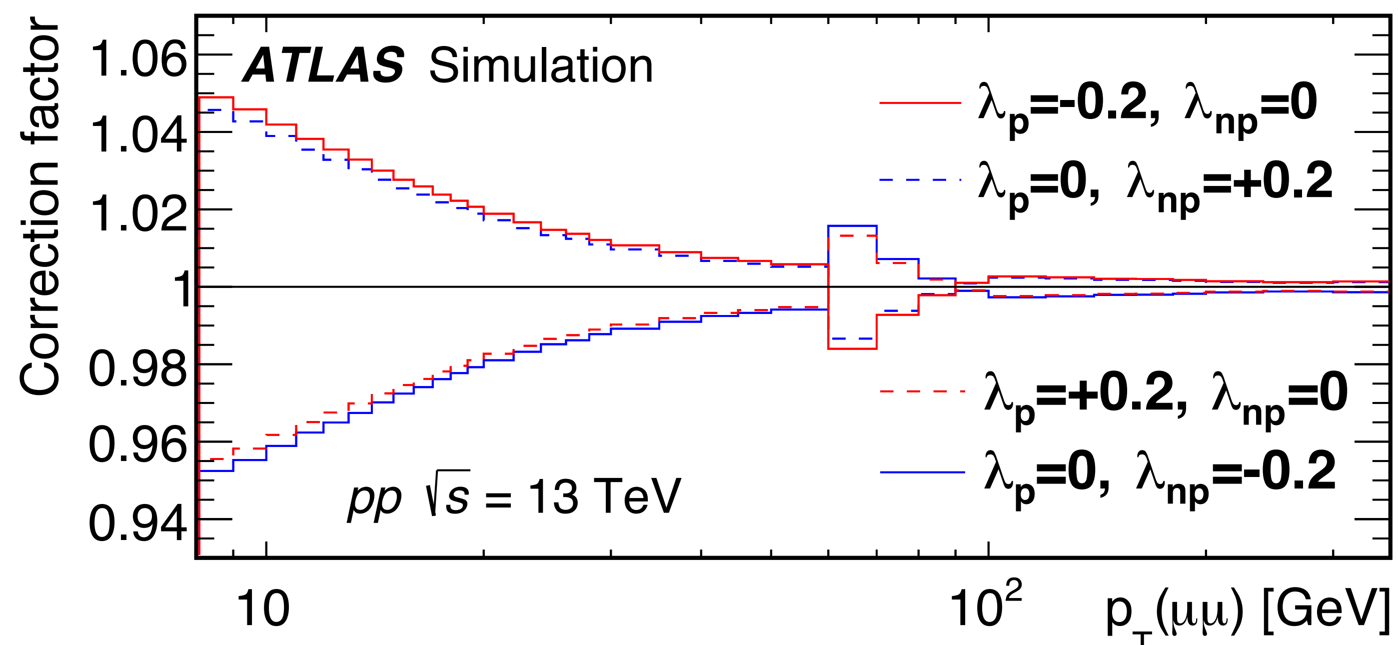

J/ψ non-prompt fraction

Compare to theory prediction: prompt

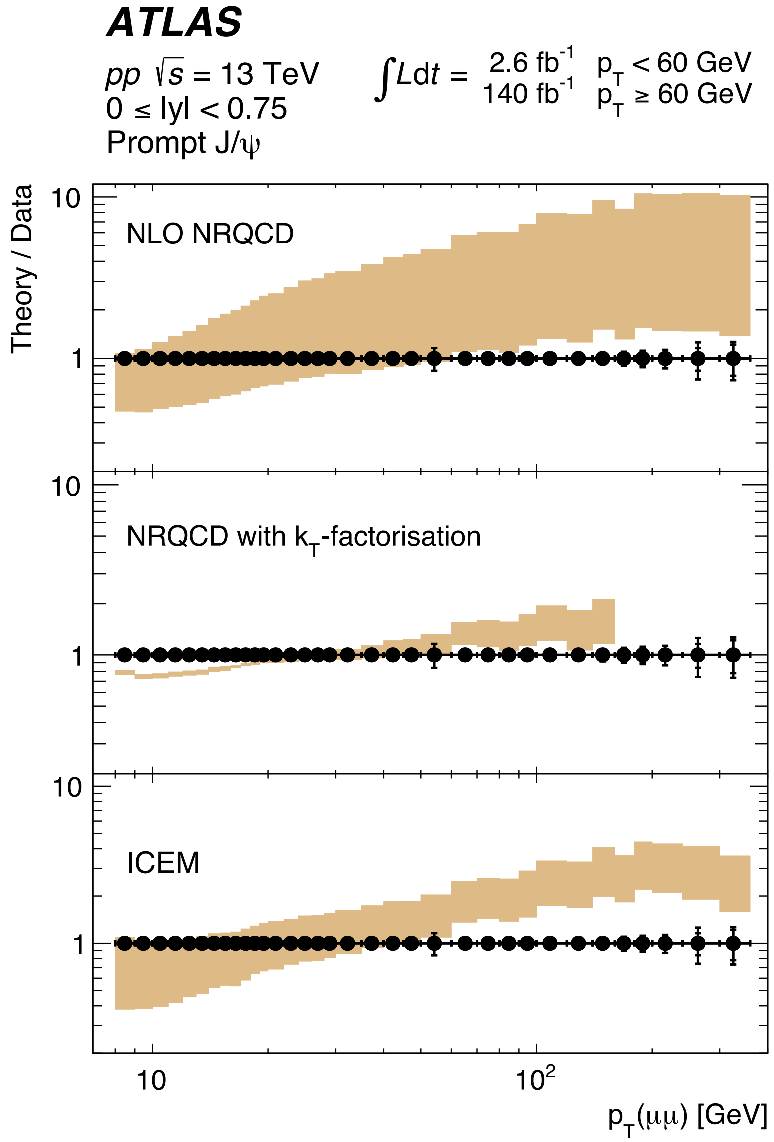

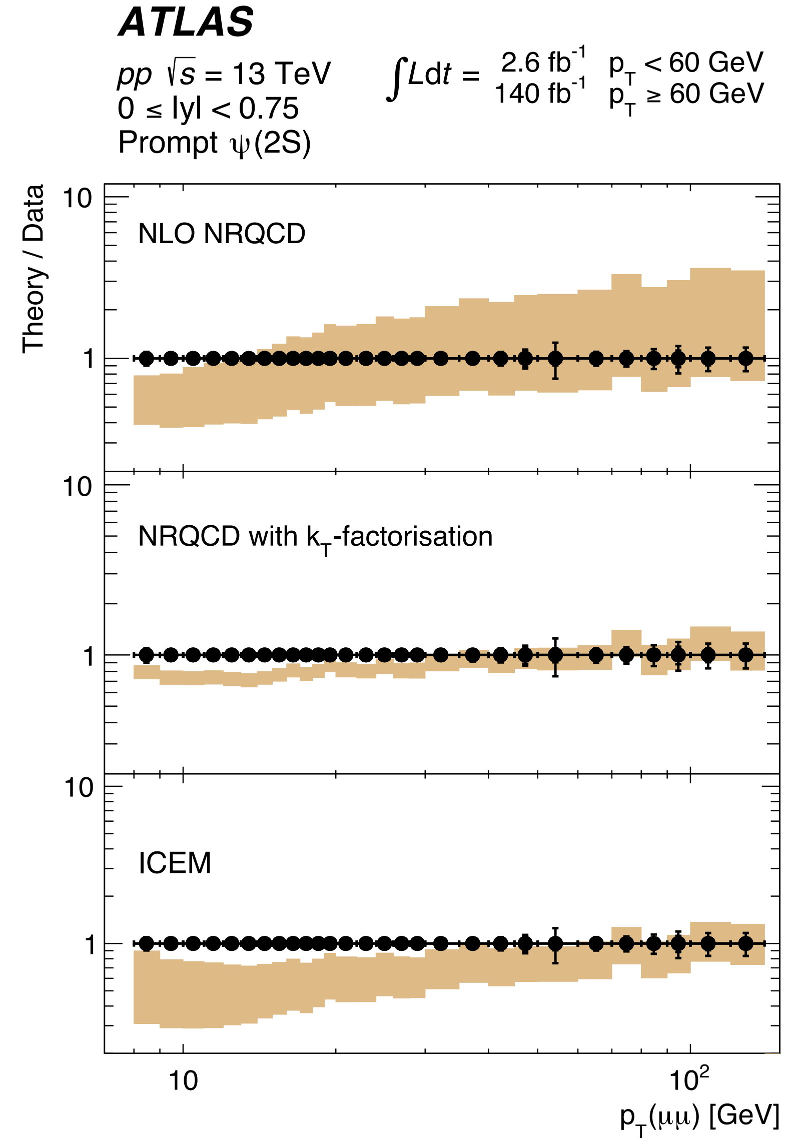

- Non-relativistic QCD approach at next-to-leading order (NLO NRQCD) —> overestimate at high p_T
- NRQCD + transverse degrees of freedom of the initial gluons in the colliding protons (k_T -factorisation model) —> underestimate at low p_T
- Improved Colour Evaporation Model (ICEM) —> harder p_T predcition for both J/ψ and $\psi(2S)$ and underestimate $\psi(2S)$ at low p_T

Compare to theory prediction: non-prompt

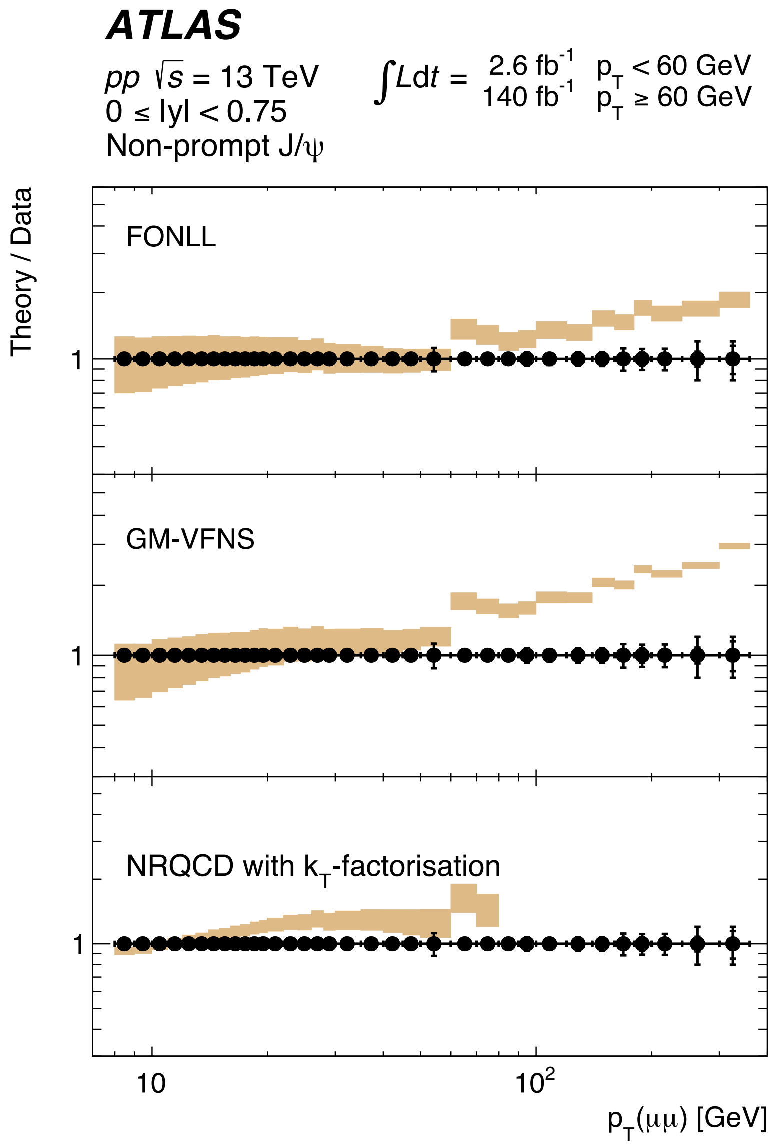

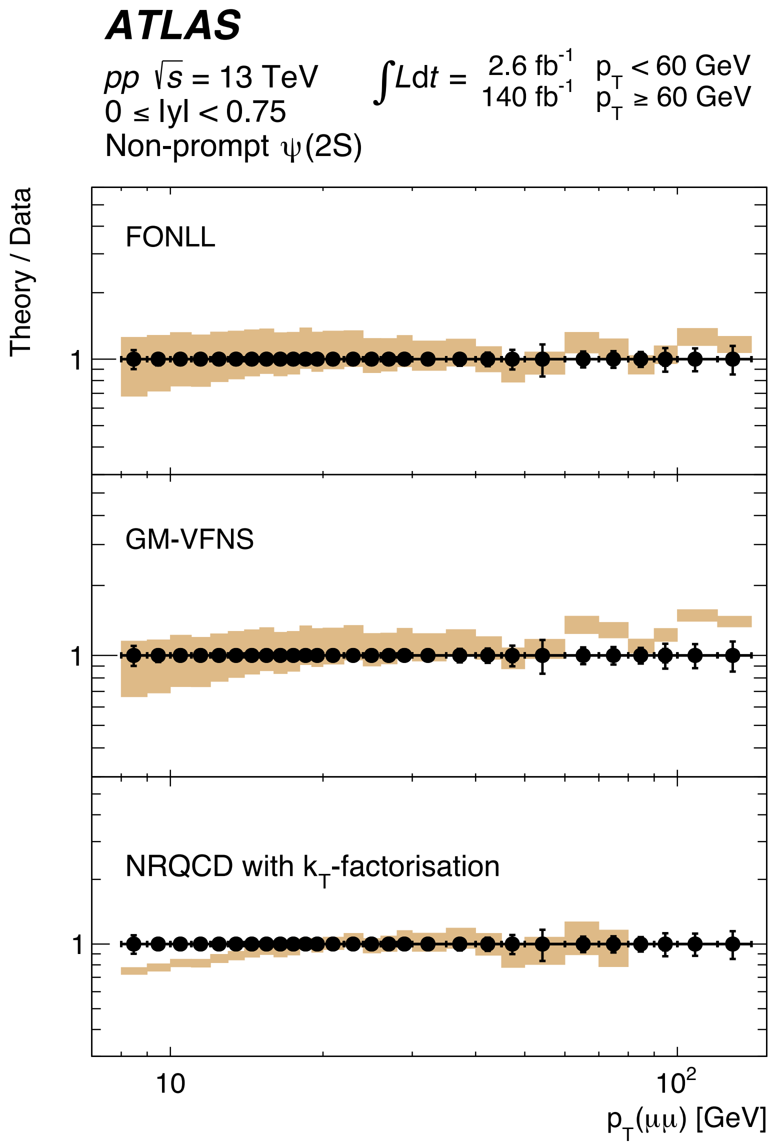

- Fixed-order–next-to-leading-log (FONLL) QCD —> good agreement at low p_T, but overestimate J/ψ at high p_T
- General-mass–variable-flavour- number scheme (GM–VFNS) —> similar results as FONLL
- NRQCD model with k_T-factorisation —> underestimate $\psi(2S)$ at low p_T

Introduction

- The quark model was proposed by Gell-Mann and Zweig sixty years ago

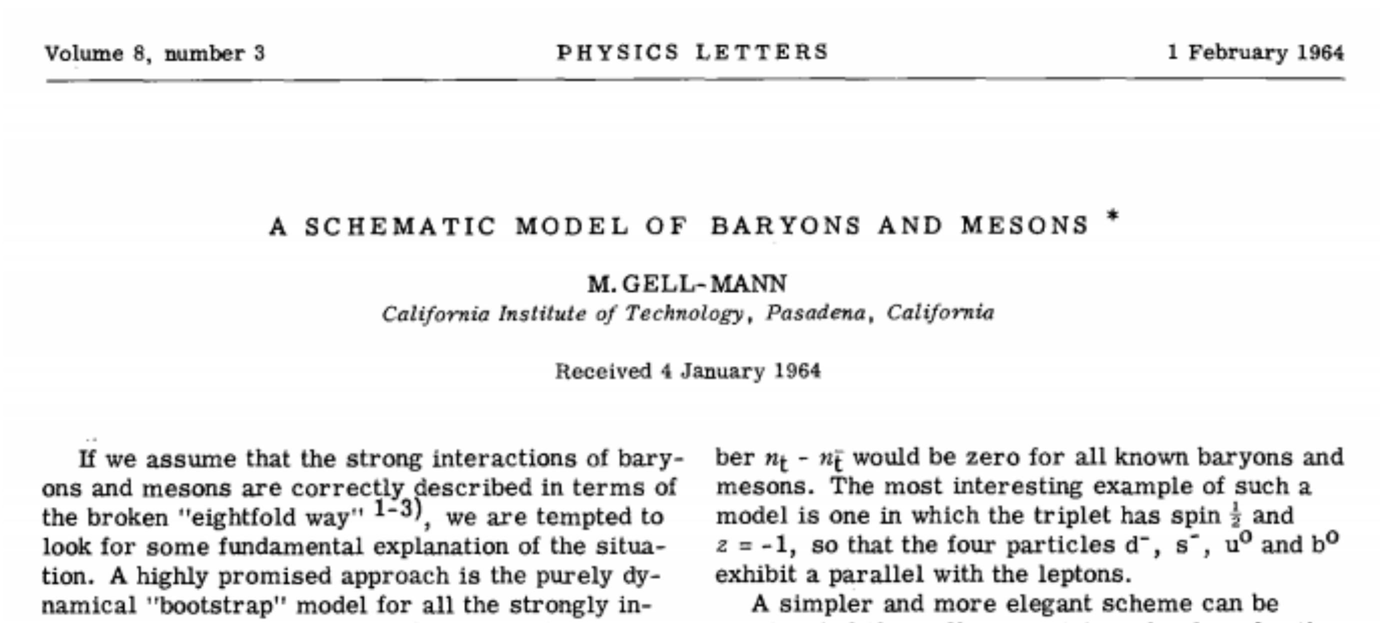

Volume 8, number 3 PHYSICS LETTERS 1 February 1964

A SCHEMATIC MODEL OF BARYONS AND MESONS *

M. GELL-MANN
California Institute of Technology, Pasadena, California

Received 4 January 1964

If we assume that the strong interactions of baryons and mesons are correctly described in terms of the broken "eightfold way" 1-3), we are tempted to look for some fundamental explanation of the situation. A highly promised approach is the purely dynamical "bootstrap" model for all the strongly in-

ber $n_t - n_{\bar{t}}$ would be zero for all known baryons and mesons. The most interesting example of such a model is one in which the triplet has spin $\frac{1}{2}$ and $z = -1$, so that the four particles d^-, s^-, u^0 and b^0 exhibit a parallel with the leptons.

A simpler and more elegant scheme can be

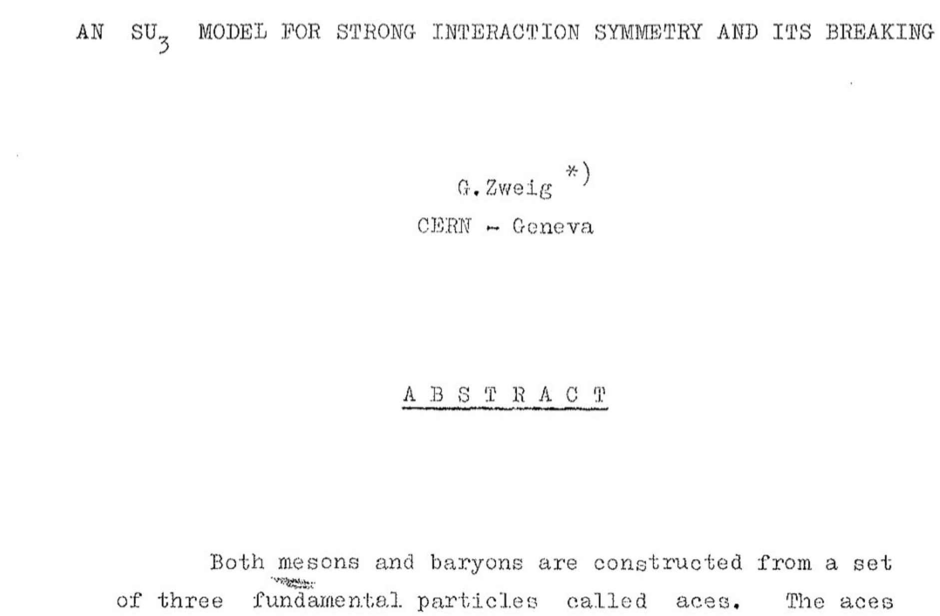

AN SU_3 MODEL FOR STRONG INTERACTION SYMMETRY AND ITS BREAKING

G. Zweig *)
CERN - Geneva

ABSTRACT

Both mesons and baryons are constructed from a set of three fundamental particles called aces. The aces

- Exotic hadrons were predicted at the same time as conventional $q\bar{q}$ mesons and qqq baryons.

Glueball

Hybrid meson

Tetraquark

Pentaquark

Observation of 4μ resonances

<table>
<tr><th>Signal region</th><th>Control region</th><th>Non-prompt region</th></tr>
<tr><td colspan="3">Di-muon or tri-muon triggers, oppositely charged muons from each charmonium,
loose muons, $p_{\mathrm{T}}^{1,2,3,4} > 4, 4, 3, 3$ GeV and $|\eta_{1,2,3,4}| < 2.5$ for the four muons,
$m_{J/\psi} \in [2.94, 3.25]$ GeV, or $m_{\psi(2S)} \in [3.56, 3.80]$ GeV,
Loose vertex requirements $\chi^2_{4\mu}/N < 40$ ($N = 5$) and $\chi^2_{\text{di-}\mu}/N < 100$ ($N = 2$),</td></tr>
<tr><td colspan="2">Vertex $\chi^2_{4\mu}/N < 3$, $L_{xy}^{4\mu} < 0.2$ mm, $|L_{xy}^{\text{di-}\mu}| < 0.3$ mm, $m_{4\mu} < 11$ GeV,</td><td rowspan="2">Vertex $\chi^2_{4\mu}/N > 6$,
or $|L_{xy}^{\text{di-}\mu}| > 0.4$ mm</td></tr>
<tr><td>$\Delta R < 0.25$ between charmonia</td><td>$\Delta R \geq 0.25$ between charmonia</td></tr>
</table>

Observation of 4μ resonances

Pseudo-proper decay time

$$\tau = L_{xy} m(\mu\mu)/p_{\mathrm{T}}(\mu\mu), \text{where } L_{xy} \equiv \mathbf{L}\cdot\mathbf{p}_{\mathrm{T}}(\mu\mu)/p_{\mathrm{T}}(\mu\mu)$$

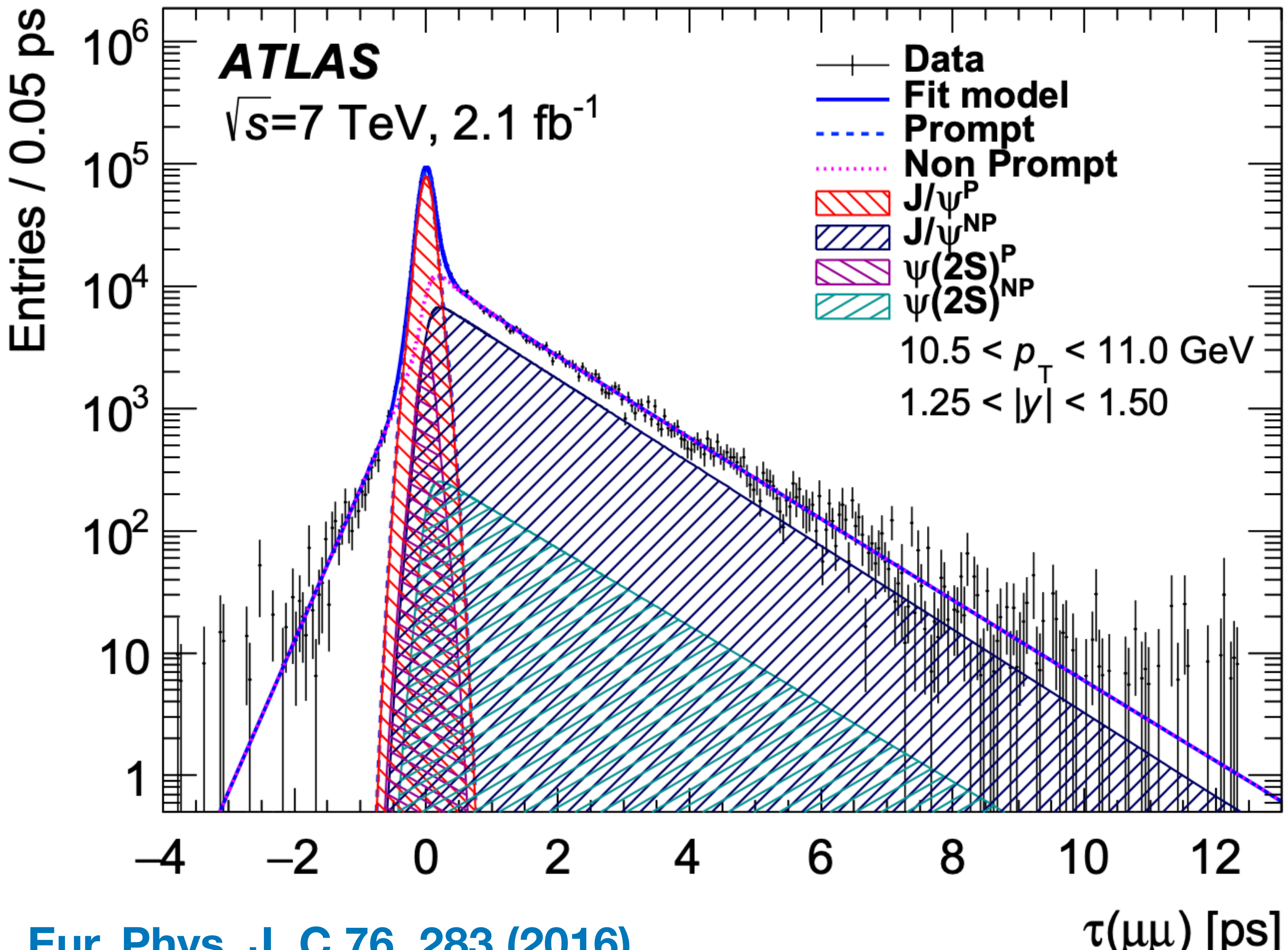

[Eur. Phys. J. C 76, 283 (2016)]

Observation of 4μ resonances

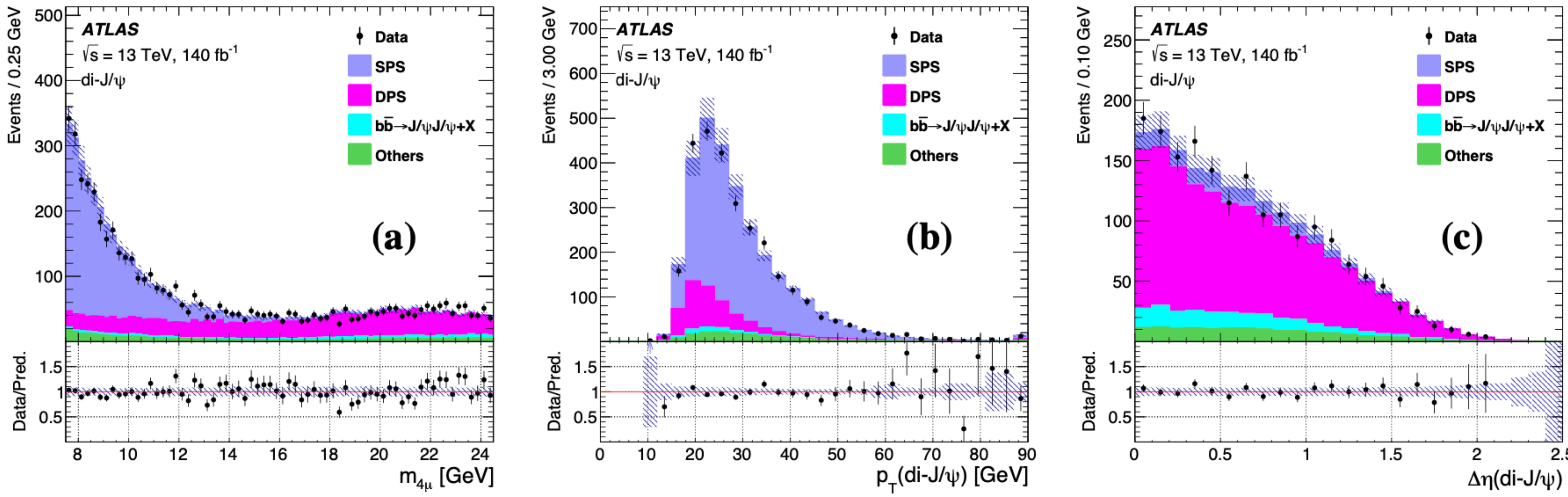

Figure 4: The 4μ mass spectrum within [7.5, 24.5] GeV and without the ΔR requirement (a), p_{T} of the di-charmonium in the SPS control region with 7.5 GeV $< m_{4\mu} <$ 12.0 GeV (b), and $\Delta\eta$ between the charmonia in the DPS control region with 14.0 GeV $< m_{4\mu} <$ 24.5 GeV (c), in the di-J/ψ channel.

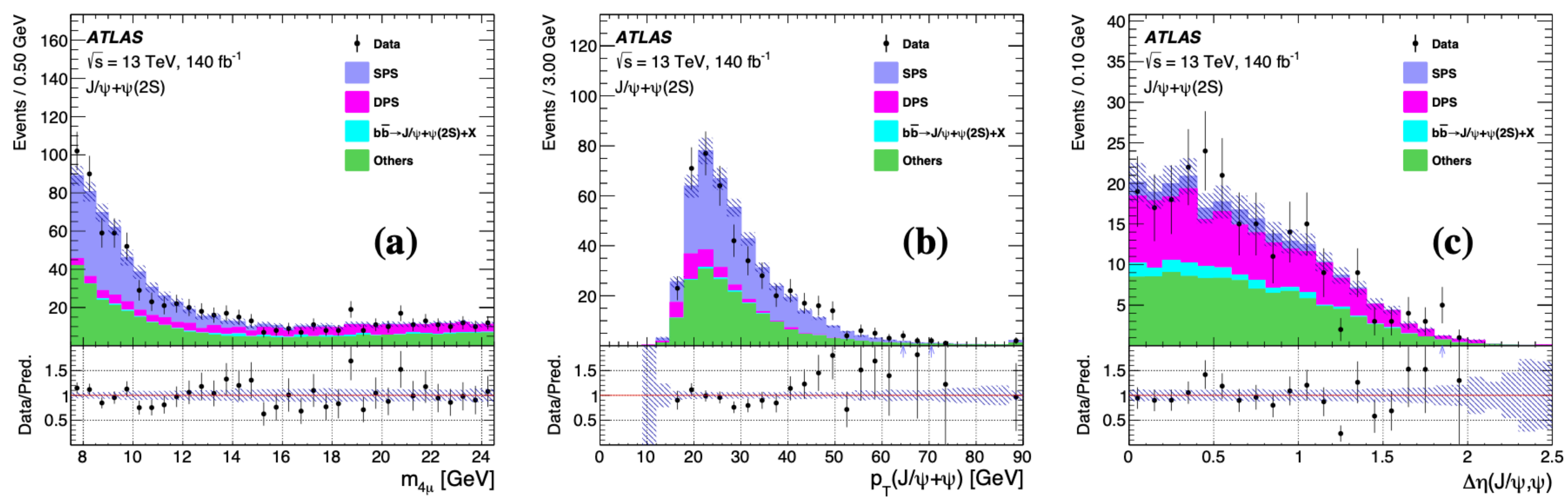

Figure 5: The 4μ mass spectrum within [7.5, 24.5] GeV and without the ΔR requirement (a), p_{T} of the di-charmonium in the SPS control region with 7.5 GeV $< m_{4\mu} <$ 12.0 GeV (b), and $\Delta\eta$ between the charmonia in the DPS control region with 14.0 GeV $< m_{4\mu} <$ 24.5 GeV (c), in the J/ψ+$\psi(2S)$ channel.

Observation of 4μ resonances

- Unbinned maximum likelihood fits are performed

$$\mathcal{L} = \mathcal{L}_{SR}\left(\vec{\alpha}, \vec{\beta}\right) \cdot \mathcal{L}_{CR}\left(\vec{\alpha}\right) \cdot \prod_{j=1}^{K} G\left(\alpha'_j; \alpha_j, \sigma_j\right)$$

- Fit regions:
  - Fit signal region (SR): $m_{4\mu}^{\text{con}} < 11$ GeV and $\Delta R < 0.25$
  - Fit control region (CR): $m_{4\mu}^{\text{con}} < 11$ GeV and $\Delta R \geq 0.25$

- The signal probability density function consists of several interfering S-wave Breit-Wigner (BW) resonances multiplied with a phase space factor and convolved with a mass resolution function.

di-J/ψ : $f_s(x) = \left| \sum_{i=0}^{2} \frac{z_i}{m_i^2 - x^2 - i m_i \Gamma_i(x)} \right|^2 \sqrt{1 - \frac{4m_{J/\psi}^2}{x^2}} \otimes R(\alpha)$

$$BW(x; m_0, \Gamma_0) = \frac{1}{m_0^2 - x^2 - i m_0 \Gamma(x)} = \frac{1}{m_0^2 - x^2 - i m_0 \Gamma_0 \frac{m_0}{x} \sqrt{\frac{x^2 - 4m_{J/\psi}^2}{m_0^2 - 4m_{J/\psi}^2}}}.$$

$J/\psi + \psi(2S)$: $f_s(x) = \left(\left| \sum_{i=0}^{2} \frac{z_i}{m_i^2 - x^2 - i m_i \Gamma_i(x)} \right|^2 + \left| \frac{z_3}{m_3^2 - x^2 - i m_3 \Gamma_3(x)} \right|^2 \right) \sqrt{1 - \left(\frac{m_{J/\psi} + m_{\psi(2S)}}{x} \right)^2} \otimes R(\alpha)$

$$\Gamma_3(x) = \Gamma_3 \frac{m_3}{x} \sqrt{\frac{x^2 - (m_{J/\psi} + m_{\psi(2S)})^2}{m_3^2 - (m_{J/\psi} + m_{\psi(2S)})^2}}.$$

Systematic uncertainties

- Only systematics affecting the mass spectrum shape are relevant

Systematic Uncertainties (MeV)	di-J/ψ m_2	di-J/ψ Γ_2	J/ψ+$\psi(2S)$ m_3	J/ψ+$\psi(2S)$ Γ_3
Muon calibration	± 6	± 7	<1	± 1
SPS model parameter	± 7	± 7	<1	
SPS di-charmonium p_T	± 7	± 8	<1	
Background MC sample size	± 7	± 8	± 1	<1
Mass resolution	± 4	-3	-1	$^{+2}_{-4}$
Fit bias	-13	$+10$	$^{+9}_{-10}$	$^{+50}_{-16}$
Shape inconsistency	<1		± 4	± 6
Transfer factor	—		± 5	± 23
Presence of 4th resonance	<1		—	
Feed-down	$^{+4}_{-1}$	$^{+6}_{-2}$	—	
Interference of 4th resonance	—		-32	-11
P and D-wave BW	$+9$	$+19$	<1	± 1
ΔR and muon p_T requirements	$^{+3}_{-2}$	$^{+6}_{-4}$	$^{+1}_{-2}$	-2
Lower resonance shape	—		$^{+3}_{-7}$	$^{+31}_{-34}$

X(6900) from LHCb

- At June 2020, LHCb claimed evidence for a narrow resonance in the di-J/Psi to 4 muons spectrum at **6.9 GeV**, presumably coming from 4-charm quark state.

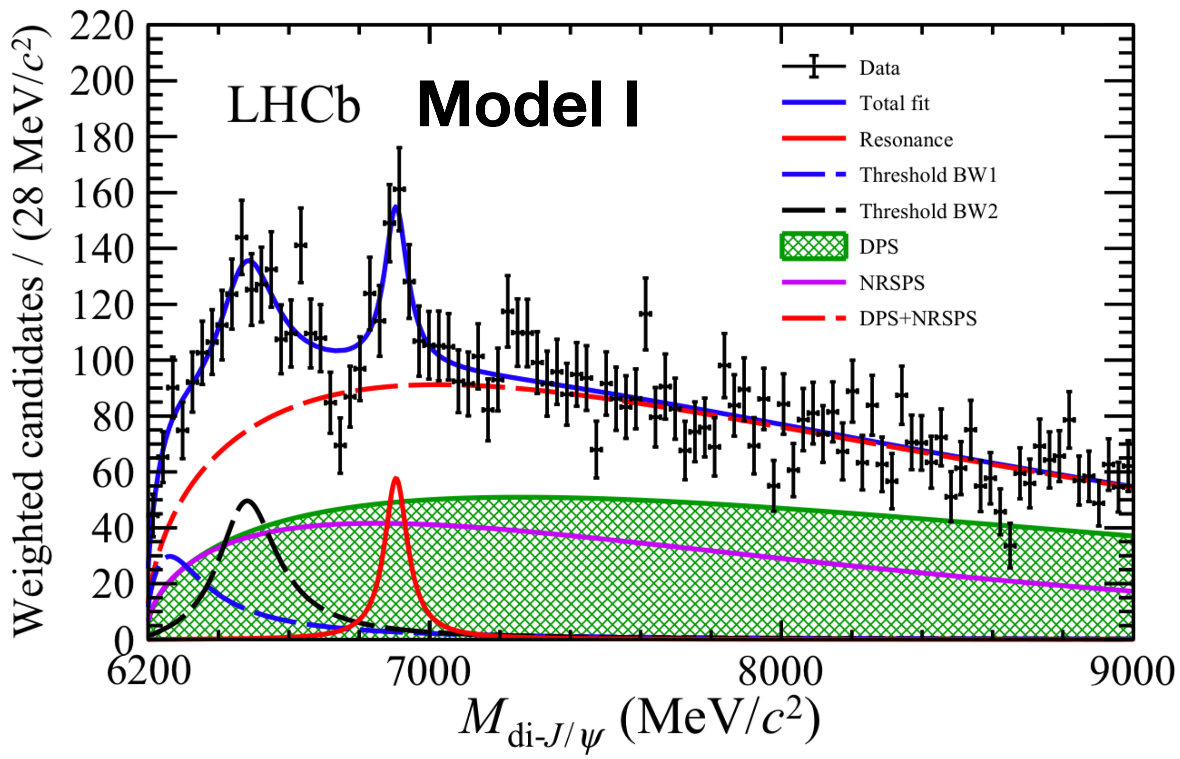

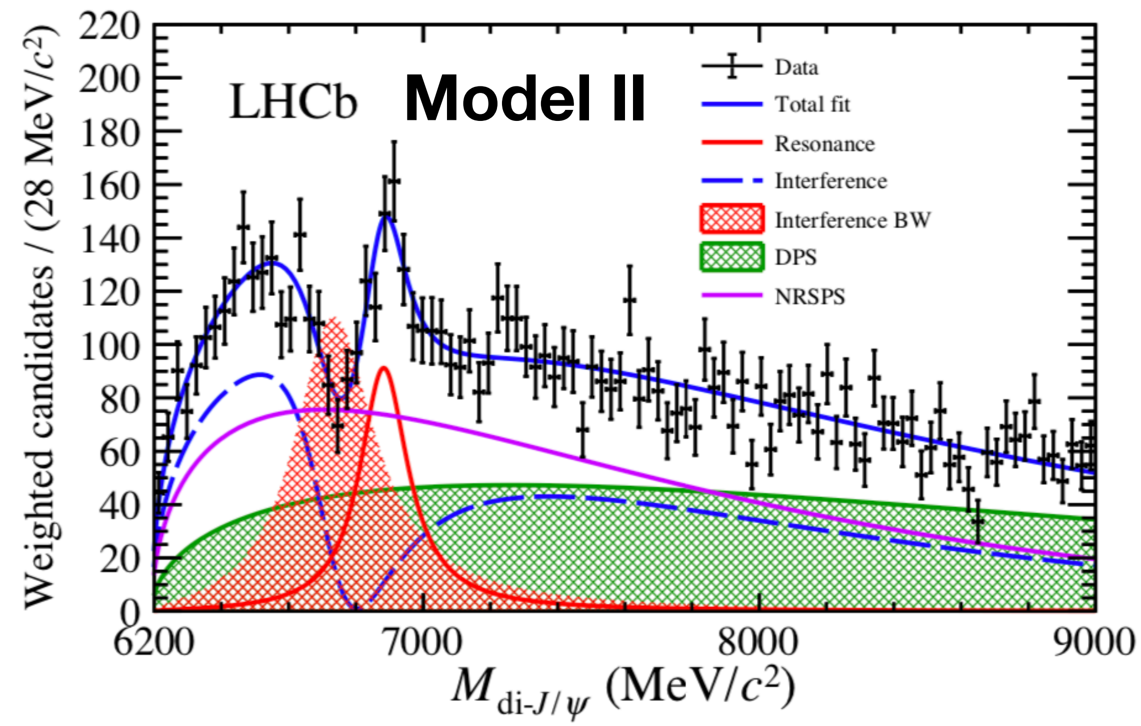

arXiv:2006.16957

LHCb model I: no interference	$m[X(6900)] = 6905 \pm 11 \pm 7\,\text{MeV}/c^2$ $\Gamma[X(6900)] = 80 \pm 19 \pm 33\,\text{MeV}$
LHCb model II: interference	$m[X(6900)] = 6886 \pm 11 \pm 11\,\text{MeV}/c^2$ $\Gamma[X(6900)] = 168 \pm 33 \pm 69\,\text{MeV}$

HL-LHC

LHC / HL-LHC Plan